Math. & Comput. Sci., 7(2) (2026), 238–264

Online: ISSN 2717-2708

Mathematics and Computational Sciences

Journal Homepage: http://mcs.qut.ac.ir/mcs

Similarity measures for complex Fermatean fuzzy sets and their applications in decision-making and clustering problems

Nisha Devi Gunasegaran[a], Hemavathi Perumal[a,*], Vinod Kumar Raja[b], Suresh Kandhasamy[c]

[a]*Department of Mathematics, Saveetha Institute of Medical and Technical Sciences (SIMATS), Saveetha School of Engineering, Thandalam, India.*

[b]*Department of Mathematics, Rajalakshmi Engineering College (Autonomous), Thandalam, India.*

[c]*Department of Mathematics, St. Joseph's College of Engineering, Chennai, India.*

Abstract

The quantification of similarity between fuzzy objects plays a crucial role in decision-making and clustering under uncertainty. Although numerous similarity measures have been developed within intuitionistic, Pythagorean, and Fermatean fuzzy frameworks, these approaches cannot be directly extended to Complex Fermatean Fuzzy Sets (CFFSs), as CFFSs represent membership and non-membership degrees using complex amplitudes and phase components. To address this limitation, the present study introduces novel similarity measures specifically designed for CFFSs, establishes their fundamental mathematical properties, and validates their effectiveness through applications in decision-making and clustering. The results demonstrate that the proposed measures effectively capture complex-valued uncertainty and provide a robust foundation for practical fuzzy analysis.

Keywords: Complex Fermatean fuzzy Sets, Similarity measure, Decision-making, Clustering.

2020 MSC: 03E72, 62H30, 90B50, 68T37, 94D05, 54H25

1. Introduction

The development of distance and similarity measures plays a fundamental role in the analysis of fuzzy sets and their extensions. Classical metrics such as Hamming, Euclidean, and Hausdorff have been widely applied within intuitionistic, picture, and Fermatean fuzzy environments to quantify uncertainty and enhance multi-criteria decision-making [12, 6, 5, 10]. These measures provide mathematical tools for evaluating the closeness between fuzzy objects, thereby supporting ranking, classification, and clustering tasks.

With the evolution of fuzzy theories, several generalized frameworks have been introduced to improve representational flexibility. Intuitionistic Fuzzy Sets (IFSs) incorporate membership and non-membership

*Corresponding author

Email addresses: nishadevig9005.sse@saveetha.com (Nisha Devi Gunasegaran), hemavathip.sse@saveetha.com (Hemavathi Perumal), vinodkumar.r@rajalakshmi.edu.in (Vinod Kumar Raja), suresh4maths@gmail.com (Suresh Kandhasamy)

doi: 10.30511/mcs.2026.2078363.1638

Received: 19 November 2025 Accepted: 14 May 2026

degrees, while Pythagorean Fuzzy Sets (PFSs) further relax constraints by allowing the squared sum of these degrees to remain within unity [19]. Fermatean Fuzzy Sets (FFSs), proposed by Senapati and Yager [16], extend this flexibility by permitting the cubic sum condition, enabling richer modeling of uncertainty. Numerous similarity and distance measures for FFSs have since been developed, including cosine, Hellinger, triangular divergence, and Tanimoto-based measures [17, 11, 18].

Parallel developments in complex-valued fuzzy frameworks have expanded the ability to represent periodic and phase-dependent information. Complex Fuzzy Sets (CFSs) and Complex Intuitionistic Fuzzy Sets (CIFSs) were introduced to incorporate amplitude and phase components [3, 7]. Complex Pythagorean Fuzzy Sets (CPFSs) further generalized these ideas, leading to advanced similarity and aggregation operators for decision-making applications [21, 1, 15]. Although these models enhance expressive capability, they still impose structural limitations inherited from their real-valued counterparts.

Recent research has focused on improving aggregation and distance modeling in fuzzy decision-making. For example, Anandarajan and John Robinson [2] proposed a neural network-based aggregation framework for complemented linguistic intuitionistic fuzzy sets, while Abbasi Shureshjani et al. [14] developed a parametric distance measure for trapezoidal intuitionistic fuzzy numbers in group decision-making contexts. These contributions strengthen fuzzy aggregation and distance analysis but remain confined to real-valued or partially complex environments.

Recent advancements have also been reported by Zeeshan et al. [22], Zhao et al. [23], Kahn and Khan [9], Nguyen et al. [13], and Arora et al. [4], who extended similarity modeling to orthopair and Q-rung fuzzy environments.

Despite these advances, similarity measures specifically tailored to Complex Fermatean Fuzzy Sets (CFFSs) remain largely unexplored. CFFSs combine the cubic flexibility of FFSs with complex-valued amplitude phase representation, offering enhanced capability for modeling dynamic and oscillatory uncertainty. However, existing similarity measures from FFSs, CPFSs, or CIFSs cannot be directly extended to CFFSs due to the simultaneous consideration of magnitude and phase information.

To address this gap, the present study develops four novel similarity measures for CFFSs -Absolute, Squared, Maximum, and Root Mean Cube formulations along with their weighted and multi-dimensional extensions. The proposed measures are rigorously validated through boundedness, symmetry, separability, and triangular inequality properties, and their effectiveness is demonstrated in decision-making and clustering applications.

1.1. Methods of CFFS

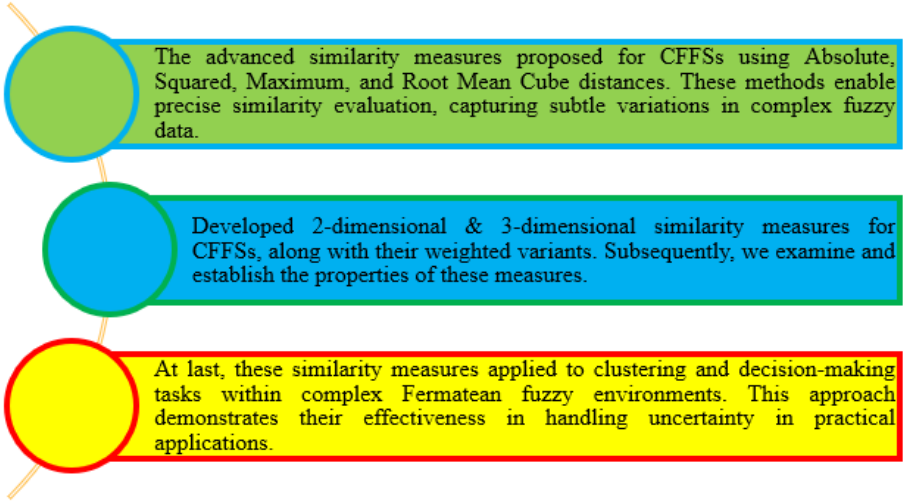

1.2. Contribution of this work

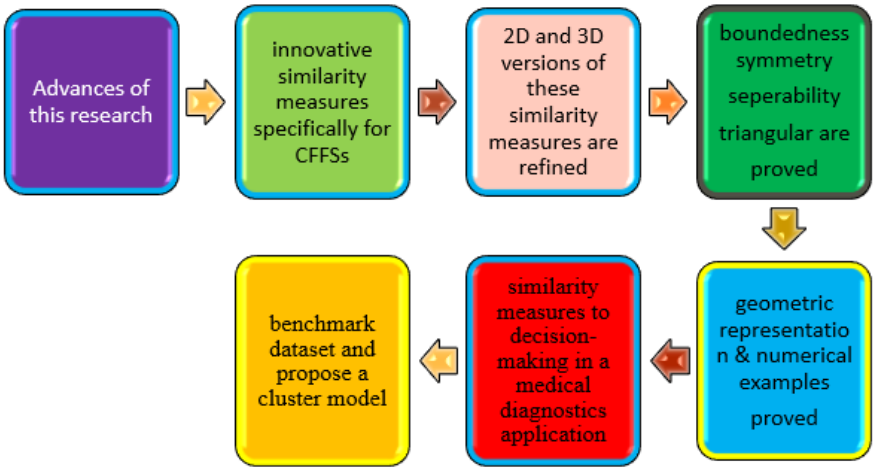

The contribution of this study can be summarized as follows:

- Development of New Similarity Measures: This study proposes new similarity measures specifically designed for Complex Fermatean Fuzzy Sets (CFFSs), addressing the limitations of existing approaches and providing a robust framework for comparing complex-valued fuzzy information.
- Rigorous Theoretical Validation: Each proposed similarity measure is supported by formal proofs to ensure mathematical consistency, boundedness, symmetry, separability, and adherence to established fuzzy-theoretic principles.
- Comprehensive Numerical Analysis: Detailed numerical analyses are conducted to compare the proposed measures with existing similarity measures, demonstrating their improved discrimination capability and stability across various scenarios.
- Applications in Decision-Making and Clustering: The practical applicability of the proposed measures is demonstrated through decision-making and clustering case studies, validating their effectiveness in real-world uncertain environments.
- Methodological Advancement of CFFSs: By extending similarity modeling to the CFFSs framework, this study enhances both the theoretical foundation and practical applicability of complex fuzzy systems.
- Implications and Future Research Directions: The concluding section discusses the strengths of the proposed measures and outlines potential avenues for future research in fuzzy algebra and complex-valued fuzzy modeling.

Overall, this work contributes to the advancement of fuzzy set theory by providing both theoretical insights and practical tools within the CFFSs framework.

1.3. Novelty and Mathematical significance

Despite recent advancements in similarity and distance measures within Fermatean and complex fuzzy environments, a systematic framework for similarity evaluation in Complex Fermatean Fuzzy Sets (CFFSs) remains underdeveloped. Most existing studies focus either on distance measures or on real-valued Fermatean fuzzy structures without fully incorporating the interaction between amplitude and phase components.

The novelty of the present study lies in the following aspects:

- Development of Four Structured Similarity Measures: Four distinct similarity formulations Absolute, Squared, Maximum, and Root Mean Cube are newly developed specifically for Complex Fermatean Fuzzy Sets. Unlike existing approaches, these measures simultaneously account for amplitude and phase variations under the Fermatean constraint.
- Unified Theoretical Validation: The proposed measures are rigorously validated by proving fundamental properties including boundedness, symmetry, separability, and triangular inequality within the CFFS framework.
- Multi-Dimensional Extensions: Two-dimensional and three-dimensional similarity formulations, along with weighted variants, are introduced to enhance modeling flexibility and general applicability.
- Integrated Application Framework: The proposed similarity measures are systematically applied to both multi-criteria decision-making and clustering problems, demonstrating their discriminative capability and robustness in practical scenarios, including medical diagnostic applications.

To the best of our knowledge, this is the first comprehensive study that develops multiple structured similarity measures with rigorous theoretical support and integrated applications specifically for Complex Fermatean Fuzzy Sets.

1.4. Framework of this work

This paper is structured to present a clear and logical progression of concepts and contributions. Section 2 reviews the fundamental concepts and preliminaries related to Complex Fermatean Fuzzy Sets (CFFSs). Section 3 introduces the proposed similarity measures and establishes their validity through rigorous mathematical proofs. Section 4 presents numerical analyses to evaluate and compare the performance of the proposed measures with existing approaches. Section 5 demonstrates their practical applicability in decision-making and clustering scenarios. Section 6 provides a detailed comparative analysis to highlight the strengths and limitations of the proposed measures. Section 7 discusses the obtained results and their practical implications. Finally, Section 8 concludes the study by summarizing the key findings and outlining directions for future research.

2. Preliminaries

This section presents the fundamental definitions and illustrative examples of Complex Fermatean Fuzzy Sets (CFFSs), along with essential concepts related to Fuzzy Sets (FSs), Fermatean Fuzzy Sets (FFSs), and similarity measures.

Definition 2.1. [20] Let $\wp$ be a universal set. A fuzzy set $\mathbf{A}$ in $\wp$ is defined as

$$\mathbf{A} = \{\langle x, \mu_{\mathbf{A}}(x)\rangle \mid x \in \wp\}$$

where the membership function $\mu_{\mathbf{A}} : \wp \to [0,1]$. For each $x \in \wp$, the value $\mu_{\mathbf{A}}(x)$ is called the membership value of x.

Definition 2.2. [8] Let $\wp = \{x_1, \ldots, x_n\}$ be a universe of discourse (UOD). An intuitionistic fuzzy set (IFS) $\mathbf{I}$ in $\wp$ is defined as $\mathbf{I} = \{\langle x, A_{\mathbf{I}}(x), B_{\mathbf{I}}(x)\rangle \mid x \in \wp\}$, where $A_{\mathbf{I}}, B_{\mathbf{I}} : \wp \to [0,1]$. For each $x \in \wp$, $A_{\mathbf{I}}(x)$ and $B_{\mathbf{I}}(x)$ represent the membership and non-membership degrees of x, respectively, satisfying $A_{\mathbf{I}}(x) + B_{\mathbf{I}}(x) \leqslant 1$. The hesitancy degree associated with $x \in \wp$ is given by $G_{\mathbf{I}}(x) = 1 - A_{\mathbf{I}}(x) - B_{\mathbf{I}}(x)$, where $G_{\mathbf{I}} : \wp \to [0,1]$.

Definition 2.3. [3] Let $\wp$ be a universal set. A Complex Intuitionistic Fuzzy Set (CIFS) $\mathbf{C}$ in $\wp$ is defined as $\mathbf{C} = \{\langle x, A_{\mathbf{C}}(x), B_{\mathbf{C}}(x)\rangle \mid x \in \wp\}$, where $A_{\mathbf{C}}, B_{\mathbf{C}} : \wp \to \{z \in \mathbf{C} \mid |z| \leqslant 1\}$, represent the complex-valued membership and non-membership degrees of x, respectively. These are expressed as $A_{\mathbf{C}}(x) = T_{\mathbf{C}}(x)e^{2\pi i W_{T_C}(x)}$, $B_{\mathbf{C}}(x) = F_{\mathbf{C}}(x)e^{2\pi i W_{F_C}(x)}$, where $T_{\mathbf{C}}(x), F_{\mathbf{C}}(x) \in [0,1]$, $\quad T_{\mathbf{C}}(x) + F_{\mathbf{C}}(x) \leqslant 1$, and

$$W_{T_C}(x), W_{F_C}(x) \in [0,1], \quad W_{T_C}(x) + W_{F_C}(x) \leqslant 1.$$

Furthermore, the hesitancy degree is represented as $G_{\mathbf{C}}(x) = R_{\mathbf{C}}(x)e^{2\pi i W_{R_C}(x)}$, where $R_{\mathbf{C}}(x) = 1 - T_{\mathbf{C}}(x) - F_{\mathbf{C}}(x)$, and $W_{R_C}(x) = 1 - W_{T_C}(x) - W_{F_C}(x)$.

Definition 2.4. [6] Let $\wp$ be a universal set. A Pythagorean fuzzy set (PFS) $\mathbf{I}$ in $\wp$ is defined as $\mathbf{I} = \{\langle x, A_{\mathbf{I}}(x), B_{\mathbf{I}}(x)\rangle \mid x \in \wp\}$, where $A_{\mathbf{I}}, B_{\mathbf{I}} : \wp \to [0,1]$ denote the membership and non-membership degrees of $x \in \wp$, respectively, satisfying $A^2_{\mathbf{I}}(x) + B^2_{\mathbf{I}}(x) \leqslant 1$. The hesitancy degree associated with $x \in \wp$ is given by $G_{\mathbf{I}}(x) = \sqrt{1 - A^2_{\mathbf{I}}(x) - B^2_{\mathbf{I}}(x)}$, where $G_{\mathbf{I}} : \wp \to [0,1]$.

Definition 2.5. [22] Let $\wp$ be a universal set. A Complex Pythagorean Fuzzy Set (CPFS) $\mathbf{C}$ in $\wp$ is defined as $\mathbf{C} = \{\langle x, A_{\mathbf{C}}(x), B_{\mathbf{C}}(x)\rangle \mid x \in \wp\}$, where $A_{\mathbf{C}}, B_{\mathbf{C}} : \wp \to \{z \in \mathbf{C} \mid |z| \leqslant 1\}$, represent the complex-valued membership and non-membership degrees, respectively. These are expressed as $A_{\mathbf{C}}(x) = T_{\mathbf{C}}(x)e^{2\pi i W_{T_C}(x)}$, $B_{\mathbf{C}}(x) = F_{\mathbf{C}}(x)e^{2\pi i W_{F_C}(x)}$, where $T_{\mathbf{C}}(x), F_{\mathbf{C}}(x) \in [0,1]$, $\quad T^2_{\mathbf{C}}(x) + F^2_{\mathbf{C}}(x) \leqslant 1$, and

$$W_{T_C}(x), W_{F_C}(x) \in [0,1], \quad W^2_{T_C}(x) + W^2_{F_C}(x) \leqslant 1.$$

Furthermore, the hesitancy degree is represented as $G_{\mathbf{C}}(x) = R_{\mathbf{C}}(x)e^{2\pi i W_{R_C}(x)}$, where

$$R_{\mathbf{C}}(x) = \sqrt{1 - T^2_{\mathbf{C}}(x) - F^2_{\mathbf{C}}(x)},$$

and $W_{R_C}(x) = \sqrt{1 - W^2_{T_C}(x) - W^2_{F_C}(x)}$.

Definition 2.6. [16] Let $\wp$ be a universal set. A Fermatean fuzzy set (FFS) $\mathbf{I}$ in $\wp$ is defined as $\mathbf{I} = \{\langle x, A_{\mathbf{I}}(x), B_{\mathbf{I}}(x)\rangle \mid x \in \wp\}$, where $A_{\mathbf{I}}, B_{\mathbf{I}} : \wp \to [0,1]$ represent the membership and non-membership degrees of $x \in \wp$, respectively, satisfying $A^3_{\mathbf{I}}(x) + B^3_{\mathbf{I}}(x) \leqslant 1$. The hesitancy degree associated with $x \in \wp$ is given by $G_{\mathbf{I}}(x) = \sqrt{1 - A^3_{\mathbf{I}}(x) - B^3_{\mathbf{I}}(x)}$, where $G_{\mathbf{I}} : \wp \to [0,1]$.

Definition 2.7. [10] Let $\wp$ be a universal set. A Complex Fermatean Fuzzy Set (CFFS) $\mathbf{C}$ in $\wp$ is defined as $\mathbf{C} = \{\langle x, A_{\mathbf{C}}(x), B_{\mathbf{C}}(x)\rangle \mid x \in \wp\}$, where $A_{\mathbf{C}}, B_{\mathbf{C}} : \wp \to \{z \in \mathbf{C} \mid |z| \leqslant 1\}$, represent the complex-valued membership and non-membership degrees, respectively. These are expressed as $A_{\mathbf{C}}(x) = T_{\mathbf{C}}(x)e^{2\pi i W_{T_C}(x)}$, $B_{\mathbf{C}}(x) = F_{\mathbf{C}}(x)e^{2\pi i W_{F_C}(x)}$, where $T_{\mathbf{C}}(x), F_{\mathbf{C}}(x) \in [0,1]$, $\quad T^3_{\mathbf{C}}(x) + F^3_{\mathbf{C}}(x) \leqslant 1$, and $W_{T_C}(x), W_{F_C}(x) \in [0,1]$, $W^3_{T_C}(x) + W^3_{F_C}(x) \leqslant 1$. Furthermore, the hesitancy degree is represented as $G_{\mathbf{C}}(x) = R_{\mathbf{C}}(x)e^{2\pi i W_{R_C}(x)}$, where $R_{\mathbf{C}}(x) = \sqrt{1 - T^3_{\mathbf{C}}(x) - F^3_{\mathbf{C}}(x)}$, and $W_{R_C}(x) = \sqrt{1 - W^3_{T_C}(x) - W^3_{F_C}(x)}$.

Definition 2.8. [15] Let $\mathbf{F} = \langle \alpha_{\mathbf{F}}, \beta_{\mathbf{F}}\rangle$ be a Fermatean fuzzy number (FFN). The score function of $\mathbf{F}$, denoted by $H(\mathbf{F})$, is defined as $H(\mathbf{F}) = \alpha^3_{\mathbf{F}} - \beta^3_{\mathbf{F}}$. Here, $H(\mathbf{F}) \in [-1,1]$.

Definition 2.9. [15] Let $\mathbf{F} = \langle \alpha_{\mathbf{F}}, \beta_{\mathbf{F}}\rangle$ be a Fermatean fuzzy number (FFN). The accuracy function of $\mathbf{F}$, denoted by $K(\mathbf{F})$, is defined as $K(\mathbf{F}) = \alpha^3_{\mathbf{F}} + \beta^3_{\mathbf{F}}$. Here, $K(\mathbf{F}) \in [0,1]$.

Definition 2.10. [6] Let $\mathbf{A} = \left\{T_{\mathbf{A}}(x)e^{2\pi i W_{T_A}(x)}, F_{\mathbf{A}}(x)e^{2\pi i W_{F_A}(x)}\right\}$ and $\mathbf{B} = \left\{T_{\mathbf{B}}(x)e^{2\pi i W_{T_B}(x)}, F_{\mathbf{B}}(x)e^{2\pi i W_{F_B}(x)}\right\}$ be two complex intuitionistic fuzzy numbers (CIFNs). Then:

1. $\mathbf{A} \subseteq \mathbf{B}$ if and only if $T_{\mathbf{A}}(x) \leqslant T_{\mathbf{B}}(x)$, $\quad F_{\mathbf{A}}(x) \geqslant F_{\mathbf{B}}(x)$, and $W_{T_A}(x) \leqslant W_{T_B}(x)$, $\quad W_{F_A}(x) \geqslant W_{F_B}(x)$.
2. $\mathbf{A} = \mathbf{B}$ if and only if $T_{\mathbf{A}}(x) = T_{\mathbf{B}}(x)$, $\quad F_{\mathbf{A}}(x) = F_{\mathbf{B}}(x)$, and $W_{T_A}(x) = W_{T_B}(x)$, $\quad W_{F_A}(x) = W_{F_B}(x)$.
3. The complement of $\mathbf{A}$ is defined as $\mathbf{A}^c = \left\{F_{\mathbf{A}}(x)e^{2\pi i W_{F_A}(x)}, T_{\mathbf{A}}(x)e^{2\pi i W_{T_A}(x)}\right\}$.

3. New Similarity Measures of Complex Fermatean Fuzzy Sets

Similarity measures can quantify the degree of similarity between two distinct alternatives. This section proposes several score-based similarity measures for CFFSs, employing the concept of distance metrics and outlining relevant properties.

1. **Universe of Discourse (UOD):** Let $\wp = \{x_1, x_2, \ldots, x_n\}$ be the universe of discourse.
2. **Complex Fermatean Fuzzy Sets (CFFSs):** Let $\mathbf{C}_1$ and $\mathbf{C}_2$ be two CFFSs defined over the same universe of discourse $\wp$. For each element $x_i \in \wp$, the membership value is characterized by a complex number. These sets are represented as

$$\mathbf{C}_1 = \left\{ \left\langle x_i, T_{\mathbf{C}_1}(x_i) e^{2\pi i W_{T_{\mathbf{C}_1}}(x_i)}, F_{\mathbf{C}_1}(x_i) e^{2\pi i W_{F_{\mathbf{C}_1}}(x_i)} \right\rangle \mid x_i \in \wp \right\},$$

$$\mathbf{C}_2 = \left\{ \left\langle x_i, T_{\mathbf{C}_2}(x_i) e^{2\pi i W_{T_{\mathbf{C}_2}}(x_i)}, F_{\mathbf{C}_2}(x_i) e^{2\pi i W_{F_{\mathbf{C}_2}}(x_i)} \right\rangle \mid x_i \in \wp \right\}.$$

3. **Membership and Non-Membership Degrees:** For each $x_i \in \wp$:
   - $T_{\mathbf{C}_1}(x_i)$, $T_{\mathbf{C}_2}(x_i)$ denote the membership degrees of x_i in $\mathbf{C}_1$ and $\mathbf{C}_2$, respectively.
   - $F_{\mathbf{C}_1}(x_i)$, $F_{\mathbf{C}_2}(x_i)$ denote the non-membership degrees of x_i in $\mathbf{C}_1$ and $\mathbf{C}_2$, respectively.
   - $W_{T_{\mathbf{C}_1}}(x_i)$, $W_{T_{\mathbf{C}_2}}(x_i)$ denote the phase terms associated with the membership degrees of x_i in $\mathbf{C}_1$ and $\mathbf{C}_2$, respectively.
   - $W_{F_{\mathbf{C}_1}}(x_i)$, $W_{F_{\mathbf{C}_2}}(x_i)$ denote the phase terms associated with the non-membership degrees of x_i in $\mathbf{C}_1$ and $\mathbf{C}_2$, respectively.

Definition 3.1 (Absolute Difference of CFFSs)**.** Let C_1 and C_2 be two complex Fermatean fuzzy sets (CFFSs) defined over $\wp = \{x_1, x_2, \ldots, x_n\}$. The absolute difference similarity measure between C_1 and C_2, denoted by $S^1_{\text{CFFSs}}(C_1, C_2)$, is defined as:

$$\begin{aligned} S^1_{\text{CFFSs}}(C_1, C_2) = 1 - \frac{1}{4n} \sum_{i=1}^{n} \Big(& \left| T^3_{C_1}(x_i) - T^3_{C_2}(x_i) + 2T_{C_1}(x_i)T_{C_2}(x_i) \right| \\ & + \left| F^3_{C_1}(x_i) - F^3_{C_2}(x_i) + 2F_{C_1}(x_i)F_{C_2}(x_i) \right| \\ & + \left| W^3_{T_{C_1}}(x_i) - W^3_{T_{C_2}}(x_i) + 2W_{T_{C_1}}(x_i)W_{T_{C_2}}(x_i) \right| \\ & + \left| W^3_{F_{C_1}}(x_i) - W^3_{F_{C_2}}(x_i) + 2W_{F_{C_1}}(x_i)W_{F_{C_2}}(x_i) \right| \Big). \end{aligned}$$

Definition 3.2 (Squared Difference of CFFSs)**.** Let C_1 and C_2 be two complex Fermatean fuzzy sets (CFFSs) defined over $\wp = \{x_1, x_2, \ldots, x_n\}$. The squared difference similarity measure between C_1 and C_2, denoted by $S^2_{\text{CFFSs}}(C_1, C_2)$, is defined as:

$$\begin{aligned} S^2_{\text{CFFSs}}(C_1, C_2) = 1 - \frac{1}{4n} \sum_{i=1}^{n} \Big(& \left(T^3_{C_1}(x_i) - T^3_{C_2}(x_i) + 2T_{C_1}(x_i)T_{C_2}(x_i) \right)^2 \\ & + \left(F^3_{C_1}(x_i) - F^3_{C_2}(x_i) + 2F_{C_1}(x_i)F_{C_2}(x_i) \right)^2 \\ & + \left(W^3_{T_{C_1}}(x_i) - W^3_{T_{C_2}}(x_i) + 2W_{T_{C_1}}(x_i)W_{T_{C_2}}(x_i) \right)^2 \\ & + \left(W^3_{F_{C_1}}(x_i) - W^3_{F_{C_2}}(x_i) + 2W_{F_{C_1}}(x_i)W_{F_{C_2}}(x_i) \right)^2 \Big). \end{aligned}$$

Definition 3.3 (Maximum Difference of CFFSs)**.** Let C_1 and C_2 be two complex Fermatean fuzzy sets (CFFSs) defined over $\wp = \{x_1, x_2, \ldots, x_n\}$. The maximum difference similarity measure between C_1 and C_2, denoted by $S^3_{\text{CFFSs}}(C_1, C_2)$, is defined as:

$$S^3_{\text{CFFSs}}(C_1, C_2) = 1 - \frac{1}{4n}\sum_{i=1}^{n} \max\Big\{ \left|T^3_{C_1}(x_i) - T^3_{C_2}(x_i) + 2T_{C_1}(x_i)T_{C_2}(x_i)\right|, \\ \left|F^3_{C_1}(x_i) - F^3_{C_2}(x_i) + 2F_{C_1}(x_i)F_{C_2}(x_i)\right|, \\ \left|W^3_{T_{C_1}}(x_i) - W^3_{T_{C_2}}(x_i) + 2W_{T_{C_1}}(x_i)W_{T_{C_2}}(x_i)\right|, \\ \left|W^3_{F_{C_1}}(x_i) - W^3_{F_{C_2}}(x_i) + 2W_{F_{C_1}}(x_i)W_{F_{C_2}}(x_i)\right| \Big\}.$$

Definition 3.4 (Root Mean Cube Difference of CFFSs)**.** Let C_1 and C_2 be two complex Fermatean fuzzy sets (CFFSs) defined over $\wp = \{x_1, x_2, \ldots, x_n\}$. The root mean cube difference similarity measure between C_1 and C_2, denoted by $S^4_{\text{CFFSs}}(C_1, C_2)$, is defined as:

$$S^4_{\text{CFFSs}}(C_1, C_2) = 1 - \frac{1}{4n}\sum_{i=1}^{n} \Bigg(\left|T^3_{C_1}(x_i) - T^3_{C_2}(x_i) + 2T_{C_1}(x_i)T_{C_2}(x_i)\right|^3 \\ + \left|F^3_{C_1}(x_i) - F^3_{C_2}(x_i) + 2F_{C_1}(x_i)F_{C_2}(x_i)\right|^3 \\ + \left|W^3_{T_{C_1}}(x_i) - W^3_{T_{C_2}}(x_i) + 2W_{T_{C_1}}(x_i)W_{T_{C_2}}(x_i)\right|^3 \\ + \left|W^3_{F_{C_1}}(x_i) - W^3_{F_{C_2}}(x_i) + 2W_{F_{C_1}}(x_i)W_{F_{C_2}}(x_i)\right|^3 \Bigg)^{\frac{1}{3}}.$$

Example 3.5 (Comparative Illustration of the Proposed Similarity Measures for CFFSs)**.** Let the universe of discourse be

$$\wp = \{x_1, x_2, \ldots, x_n\}.$$

Two complex Fermatean fuzzy sets (CFFSs) C_1 and C_2 defined over $\mathcal{P}$ are given as:

$$C_1 = \left\{ \left\langle x_i, T_{C_1}(x_i)e^{2\pi i W_{T_{C_1}}(x_i)}, F_{C_1}(x_i)e^{2\pi i W_{F_{C_1}}(x_i)} \right\rangle \;\middle|\; x_i \in \mathcal{P} \right\},$$

$$C_2 = \left\{ \left\langle x_i, T_{C_2}(x_i)e^{2\pi i W_{T_{C_2}}(x_i)}, F_{C_2}(x_i)e^{2\pi i W_{F_{C_2}}(x_i)} \right\rangle \;\middle|\; x_i \in \mathcal{P} \right\}.$$

Table 1: Numerical values of C_1 and C_2

x_i	$T_{C_1}(x_i)$	$F_{C_1}(x_i)$	$W_{T_{C_1}}(x_i)$	$W_{F_{C_1}}(x_i)$	$T_{C_2}(x_i)$	$F_{C_2}(x_i)$	$W_{T_{C_2}}(x_i)$	$W_{F_{C_2}}(x_i)$
x_1	0.7	0.2	0.3	0.1	0.6	0.3	0.4	0.2
x_2	0.8	0.1	0.4	0.2	0.7	0.2	0.5	0.1
x_3	0.6	0.3	0.2	0.2	0.5	0.4	0.3	0.3

Each pair of values $(T_{C_j}(x_i), F_{C_j}(x_i))$ satisfies the Fermatean condition:

$$T^3_{C_j}(x_i) + F^3_{C_j}(x_i) \leqslant 1, \quad j = 1, 2.$$

Using Definition 3.1:

$$S^1_{CFFSs}(C_1, C_2) = 1 - \frac{1}{4n}\sum_{i=1}^{n}\Big(\left|T^3_{C_1}(x_i) - T^3_{C_2}(x_i) + 2T_{C_1}(x_i)T_{C_2}(x_i)\right| + \left|F^3_{C_1}(x_i) - F^3_{C_2}(x_i) + 2F_{C_1}(x_i)F_{C_2}(x_i)\right| + \left|W^3_{T_{C_1}}(x_i) - W^3_{T_{C_2}}(x_i) + 2W_{T_{C_1}}(x_i)W_{T_{C_2}}(x_i)\right| + \left|W^3_{F_{C_1}}(x_i) - W^3_{F_{C_2}}(x_i) + 2W_{F_{C_1}}(x_i)W_{F_{C_2}}(x_i)\right|\Big).$$

After computation,

$$S^1_{CFFSs}(C_1, C_2) = 0.928.$$

Using Definition 3.2:

$$S^2_{CFFSs}(C_1, C_2) = 1 - \frac{1}{4n}\sum_{i=1}^{n}\Big(\left(T^3_{C_1}(x_i) - T^3_{C_2}(x_i) + 2T_{C_1}(x_i)T_{C_2}(x_i)\right)^2 + \left(F^3_{C_1}(x_i) - F^3_{C_2}(x_i) + 2F_{C_1}(x_i)F_{C_2}(x_i)\right)^2 + \left(W^3_{T_{C_1}}(x_i) - W^3_{T_{C_2}}(x_i) + 2W_{T_{C_1}}(x_i)W_{T_{C_2}}(x_i)\right)^2 + \left(W^3_{F_{C_1}}(x_i) - W^3_{F_{C_2}}(x_i) + 2W_{F_{C_1}}(x_i)W_{F_{C_2}}(x_i)\right)^2\Big).$$

After simplification,

$$S^2_{CFFSs}(C_1, C_2) = 0.942.$$

Using Definition 3.3:

$$S^3_{CFFSs}(C_1, C_2) = 1 - \frac{1}{4n}\sum_{i=1}^{n}\max\Big\{\left|T^3_{C_1}(x_i) - T^3_{C_2}(x_i) + 2T_{C_1}(x_i)T_{C_2}(x_i)\right|, \left|F^3_{C_1}(x_i) - F^3_{C_2}(x_i) + 2F_{C_1}(x_i)F_{C_2}(x_i)\right|, \left|W^3_{T_{C_1}}(x_i) - W^3_{T_{C_2}}(x_i) + 2W_{T_{C_1}}(x_i)W_{T_{C_2}}(x_i)\right|, \left|W^3_{F_{C_1}}(x_i) - W^3_{F_{C_2}}(x_i) + 2W_{F_{C_1}}(x_i)W_{F_{C_2}}(x_i)\right|\Big\}.$$

After computation,

$$S^3_{CFFSs}(C_1, C_2) = 0.915.$$

Using Definition 3.4:

$$S^4_{CFFSs}(C_1, C_2) = 1 - \frac{1}{4n}\sum_{i=1}^{n}\Bigg(\left|T^3_{C_1}(x_i) - T^3_{C_2}(x_i) + 2T_{C_1}(x_i)T_{C_2}(x_i)\right|^3 + \left|F^3_{C_1}(x_i) - F^3_{C_2}(x_i) + 2F_{C_1}(x_i)F_{C_2}(x_i)\right|^3 + \left|W^3_{T_{C_1}}(x_i) - W^3_{T_{C_2}}(x_i) + 2W_{T_{C_1}}(x_i)W_{T_{C_2}}(x_i)\right|^3 + \left|W^3_{F_{C_1}}(x_i) - W^3_{F_{C_2}}(x_i) + 2W_{F_{C_1}}(x_i)W_{F_{C_2}}(x_i)\right|^3\Bigg)^{\frac{1}{3}}.$$

After simplification,

$$S^4_{CFFSs}(C_1, C_2) = 0.936.$$

Table 2: Interpretation of the Proposed Similarity Measures

Similarity Measure	Symbol	Computed Value	Interpretation
Absolute difference	$S^1_{CFFSs}(C_1, C_2)$	0.928	Indicates high similarity with slight deviation
Squared difference	$S^2_{CFFSs}(C_1, C_2)$	0.942	Slightly smoother measure emphasizing larger deviations
Maximum difference	$S^3_{CFFSs}(C_1, C_2)$	0.915	Sensitive to the largest difference among attributes
Root mean cube difference	$S^4_{CFFSs}(C_1, C_2)$	0.936	Balances sensitivity and robustness to variation

This combined numerical example confirms that all four proposed similarity measures yield consistent and interpretable results, reflecting subtle variations in the manner they capture the complex relationships between two CFFSs. Hence, these measures are mathematically reasonable, scientifically sound, and computationally demonstrative, providing a comprehensive framework for assessing similarity in the context of Complex Fermatean Fuzzy information.

Theorem 3.6. *Let* C_1, C_2, *and* C_3 *be three CFFSs in* $\wp$. *Define the similarity measure for* $K = 1, 2, 3, 4$ *as*

$$S^K_{CFFSs}(C_1, C_2) = 1 - \frac{1}{4n} \sum_{i=1}^{n} \Phi_K\big(x_i; C_1, C_2\big),$$

where Φ_K *denotes the corresponding non-negative per-element aggregation (absolute differences for* $K = 1$, *squared differences for* $K = 2$, *maximum-type aggregation for* $K = 3$, *and* p*-norm form for* $K = 4$*). Then the following properties hold:*

1. ***(Boundedness and Non-negativity)***

$$0 \leqslant S^K_{CFFSs}(C_1, C_2) \leqslant 1, \quad \textit{for all } K.$$

2. ***(Separability)***

$$S^K_{CFFSs}(C_1, C_2) = 1 \quad \textit{if and only if} \quad C_1 = C_2.$$

3. ***(Symmetry)***

$$S^K_{CFFSs}(C_1, C_2) = S^K_{CFFSs}(C_2, C_1).$$

4. ***(Triangle-type Inequality)***

$$S^K_{CFFSs}(C_1, C_2) + S^K_{CFFSs}(C_2, C_3) \geqslant S^K_{CFFSs}(C_1, C_3), \quad \textit{for } K = 3, 4.$$

Proof. **Case 1:** (Take $\mathbf{S}^2_{CFFSs}(\mathbf{C}_1, \mathbf{C}_2)$)

$$\mathbf{S}^2_{CFFSs}(\mathbf{C}_1, \mathbf{C}_2) = 1 - \frac{1}{4n} \sum_{i=1}^{n} \Big[(d_T(x_i))^2 + (d_F(x_i))^2 + (d_{W_T}(x_i))^2 + (d_{W_F}(x_i))^2\Big],$$

where

$$d_T(x_i) = T^3_{\mathbf{C}_1}(x_i) - T^3_{\mathbf{C}_2}(x_i),$$
$$d_F(x_i) = F^3_{\mathbf{C}_1}(x_i) - F^3_{\mathbf{C}_2}(x_i),$$
$$d_{W_T}(x_i) = W^3_{T_{\mathbf{C}_1}}(x_i) - W^3_{T_{\mathbf{C}_2}}(x_i),$$
$$d_{W_F}(x_i) = W^3_{F_{\mathbf{C}_1}}(x_i) - W^3_{F_{\mathbf{C}_2}}(x_i).$$

Since all membership and non-membership values lie in $[0, 1]$, their squared differences are bounded by 1. Hence,

$$0 \leqslant \mathbf{S}^2_{CFFSs}(\mathbf{C}_1, \mathbf{C}_2) \leqslant 1.$$

Case 2: (Take $\mathbf{S}^1_{CFFSs}(\mathbf{C}_1, \mathbf{C}_2)$)

$$\mathbf{S}^1_{\mathrm{CFFSs}}(\mathbf{C}_1,\mathbf{C}_2) = 1 - \frac{1}{4n}\sum_{i=1}^{n}\Big[|d_T(x_i)| + |d_F(x_i)| + |d_{W_T}(x_i)| + |d_{W_F}(x_i)|\Big].$$

If $\mathbf{S}^1_{\mathrm{CFFSs}}(\mathbf{C}_1,\mathbf{C}_2) = 0$, then each absolute difference must be zero, which implies

$$T_{\mathbf{C}_1}(x_i) = T_{\mathbf{C}_2}(x_i), \quad F_{\mathbf{C}_1}(x_i) = F_{\mathbf{C}_2}(x_i),$$
$$W_{T_{\mathbf{C}_1}}(x_i) = W_{T_{\mathbf{C}_2}}(x_i), \quad W_{F_{\mathbf{C}_1}}(x_i) = W_{F_{\mathbf{C}_2}}(x_i).$$

Hence, $\mathbf{C}_1 = \mathbf{C}_2$.

Case 3: (Take $\mathbf{S}^3_{\mathrm{CFFSs}}$)
Since the maximum and absolute value operators are symmetric,

$$\Phi_3(x_i;\mathbf{C}_1,\mathbf{C}_2) = \Phi_3(x_i;\mathbf{C}_2,\mathbf{C}_1).$$

Therefore,

$$\mathbf{S}^3_{\mathrm{CFFSs}}(\mathbf{C}_1,\mathbf{C}_2) = \mathbf{S}^3_{\mathrm{CFFSs}}(\mathbf{C}_2,\mathbf{C}_1).$$

Case 4: (Take $\mathbf{S}^4_{\mathrm{CFFSs}}$)
By Minkowski inequality, for $p \geqslant 1$,

$$\left(\sum_{i=1}^{n} a_i^p\right)^{1/p} + \left(\sum_{i=1}^{n} b_i^p\right)^{1/p} \geqslant \left(\sum_{i=1}^{n}(a_i+b_i)^p\right)^{1/p}.$$

Applying this to the per-element cubic differences of $\mathbf{C}_1, \mathbf{C}_2, \mathbf{C}_3$, we obtain

$$\mathbf{S}^4_{\mathrm{CFFSs}}(\mathbf{C}_1,\mathbf{C}_2) + \mathbf{S}^4_{\mathrm{CFFSs}}(\mathbf{C}_2,\mathbf{C}_3) \geqslant \mathbf{S}^4_{\mathrm{CFFSs}}(\mathbf{C}_1,\mathbf{C}_3).$$

Hence, the proof is completed. □

4. Numerical Example

This section provides a step-by-step numerical illustration to validate the proposed methods or theoretical advancements. The example is designed to demonstrate the application of the developed similarity measures and their effectiveness in practical scenarios.

Example 4.1. We examine two CFFSs, denoted as $\mathbf{C}_1$ and $\mathbf{C}_2$, defined on the universal object domain $\wp$ as follows:

$$\mathbf{C}_1 = \left(\gamma e^{2\pi i\delta},\ \delta e^{2\pi i\gamma}\right),$$
$$\mathbf{C}_2 = \left(\delta e^{2\pi i\gamma},\ \gamma e^{2\pi i\delta}\right),$$

where γ and δ are real numbers in the interval $[0,1]$ satisfying the constraint

$$\gamma^3 + \delta^3 \leqslant 1.$$

The similarity measure $\mathbf{S}^2_{\mathrm{CFFSs}}$ between $\mathbf{C}_1$ and $\mathbf{C}_2$ can be computed as the parameters γ and δ vary. As γ approaches δ (i.e., $\gamma = \delta$), the distance component of $\mathbf{S}^2_{\mathrm{CFFSs}}$ tends toward 0, indicating maximal similarity between the two sets. For instance, when $\gamma = \delta = 0.5$, the value of $\mathbf{S}^2_{\mathrm{CFFSs}}$ becomes very small.

Similarly, the similarity measure $\mathbf{S}^4_{\mathrm{CFFSs}}$ follows the same pattern. When $\gamma = \delta$, the measure attains its minimum value. When $\gamma = 0$ and $\delta = 1$ (or vice versa), both $\mathbf{S}^2_{\mathrm{CFFSs}}$ and $\mathbf{S}^4_{\mathrm{CFFSs}}$ attain the maximum value of 1, indicating maximal dissimilarity.

Thus, the measures $\mathbf{S}^2_{\text{CFFSs}}$ and $\mathbf{S}^4_{\text{CFFSs}}$ vary within $[0,1]$, satisfying the boundedness and non-degeneracy properties. When $\gamma = \delta$, the CFFSs $\mathbf{C}_1$ and $\mathbf{C}_2$ are most similar, and the distance is minimal. When $\gamma = 0$ and $\delta = 1$ (or vice versa), the sets are maximally different, and the distance is maximal.

Figure 1 illustrates the overall workflow of the proposed CFFSs-based similarity-measure model, including data acquisition, normalization, CFFSs construction, computation of $\mathbf{S}^{\mathsf{K}}_{\text{CFFSs}}$ $(\mathsf{K} = 1,2,3,4)$, and final decision generation.

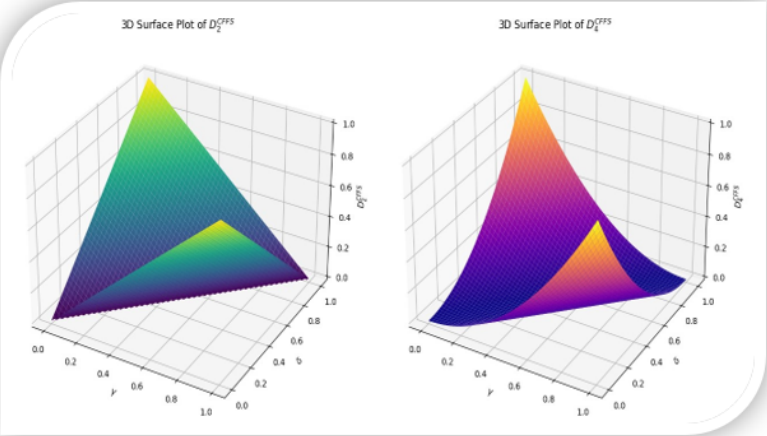

Figure 1: Similarity measures between S^2_{CFFS} and S^4_{CFFS}

Example 4.2. Let us consider three CFFSs, labelled as $\mathbf{C}_1$, $\mathbf{C}_2$, and $\mathbf{C}_3$ in the universal object domain $\wp$. The sets are characterized as follows:

$$\mathbf{C}_1 = \left(\gamma e^{2\pi i\delta},\ \delta e^{2\pi i\gamma}\right),$$

$$\mathbf{C}_2 = \left(\gamma e^{2\pi i\delta},\ \gamma e^{2\pi i\delta}\right),$$

$$\mathbf{C}_3 = \left(\gamma e^{2\pi i\gamma},\ \delta e^{2\pi i\delta}\right).$$

Now, consider the following numerical values:

$$\mathbf{C}_1 = \left(0.10\, e^{2\pi i(0.30)},\ 0.40\, e^{2\pi i(0.20)}\right),$$

$$\mathbf{C}_2 = \left(0.30\, e^{2\pi i(0.50)},\ 0.50\, e^{2\pi i(0.10)}\right),$$

$$\mathbf{C}_3 = \left(0.60\, e^{2\pi i(0.20)},\ 0.20\, e^{2\pi i(0.40)}\right).$$

These CFFSs can now be utilized to compute the similarity measures $\mathbf{S}^{\mathsf{K}}_{\text{CFFSs}}$ $(\mathsf{K} = 1,2,3,4)$ for comparative analysis.

Table 3: Computed Values of $\mathbf{S}^{K}_{CFFSs}$ for Pairwise Comparisons

K	$(\mathbf{C}_1, \mathbf{C}_2)$	$(\mathbf{C}_2, \mathbf{C}_3)$	$(\mathbf{C}_1, \mathbf{C}_3)$
1	0.7273	0.6327	0.8153
2	0.9056	0.8747	0.9714
3	0.7273	0.6327	0.8153
4	0.8421	0.8237	0.9216

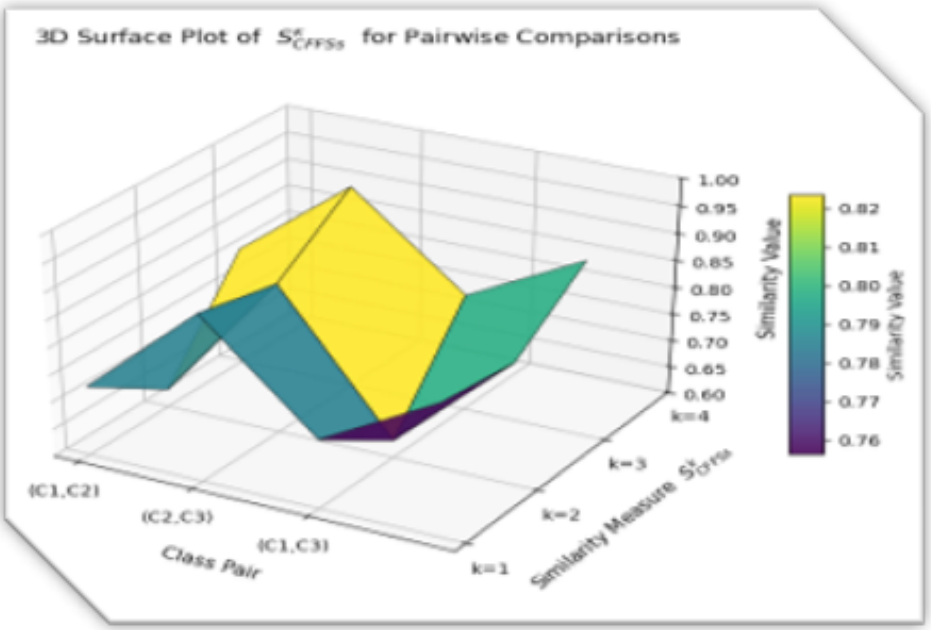

Figure 2: Fig.2. Similarity measures of 3D and 2D plots.

From the computed results, we conclude that

$$\mathbf{S}^{K}_{CFFSs}(\mathbf{C}_1, \mathbf{C}_2) + \mathbf{S}^{K}_{CFFSs}(\mathbf{C}_2, \mathbf{C}_3) \geqslant \mathbf{S}^{K}_{CFFSs}(\mathbf{C}_1, \mathbf{C}_3),$$

holds for $K = 3$ and 4. This confirms the satisfaction of the triangle inequality property within the framework of $\mathbf{S}_{CFFSs}$.

Furthermore, the 3D surface plot provides a more comprehensive visual interpretation of the relationships and variations in similarity measures across different datasets and parameter conditions compared to a traditional 2D representation.

In addition, the heatmap visualization clearly highlights variations in similarity values, enabling easy identification of combinations of $\mathbf{S}_{CFFSs}$ levels and categories that exhibit higher or lower similarities. It offers an efficient means to observe patterns, trends, and potential outliers within the datasets.

5. Practical use in decision making

This part introduces adaptive distance measures, designed to modify according to dataset features, enhancing decision-making and clustering in various real-world situations.

5.1. Problem Description

Consider a finite universe of discourse (UOD) $\wp = \{x_1, x_2, \ldots, x_n\}$, where each x_i denotes an element of the domain. Assume that there are m known patterns represented by CFFSs $\mathbf{C}_k$, $(k = 1, 2, \ldots, m)$.

The classification problem consists of assigning a new query pattern $\mathbf{C}$ to one of the known patterns $\mathbf{C}_k$ based on the proposed similarity measures.

5.2. Objective

The objective is to assign the query pattern $\mathbf{C}$ to the most similar pattern among the m predefined patterns by computing the dissimilarity between $\mathbf{C}$ and each $\mathbf{C}_k$, $(k = 1, 2, \ldots, m)$, and selecting the pattern corresponding to the minimum dissimilarity measure.

Steps for Classification

1. Use the similarity measure $\mathbf{S}^{K}_{CFFSs}$, $(K = 1, 2, 3, 4)$, to compute the dissimilarity between the query pattern $\mathbf{C}$ and each known pattern $\mathbf{C}_k$, $(k = 1, 2, \ldots, m)$. Different measures may capture different aspects of dissimilarity.
2. Determine
$$\mathbf{S}^{K}_{CFFSs}(\mathbf{C}_{k'}, \mathbf{C}) = \min_{1 \leqslant k \leqslant m} \mathbf{S}^{K}_{CFFSs}(\mathbf{C}_k, \mathbf{C}),$$
where $\mathbf{C}_{k'}$ denotes the pattern having the smallest dissimilarity to the query pattern $\mathbf{C}$. Thus, $\mathbf{C}_{k'}$ is considered the closest match.
3. Classify the query pattern $\mathbf{C}$ as belonging to the same category or class as the closest pattern $\mathbf{C}_{k'}$.
4. Compute the Degree of Confidence (DoC) to evaluate the reliability of the classification decision:
$$\text{DoC} = \sum_{\substack{k=1 \\ k \neq k'}}^{m} \left| \mathbf{S}^{K}_{CFFSs}(\mathbf{C}_k, \mathbf{C}) - \mathbf{S}^{K}_{CFFSs}(\mathbf{C}_{k'}, \mathbf{C}) \right|.$$
Here, $\mathbf{C}_{k'}$ represents the classified result corresponding to $\mathbf{C}$. A higher DoC value indicates stronger confidence and improved decision-making capability.

5.3. Application

Let us consider an alternative scenario in a medical diagnostics application where different disease types are classified based on various symptoms. In this case, CFFSs are used to model patient data over an attribute set $\boldsymbol{\sigma} = \{\sigma_1, \sigma_2, \sigma_3, \sigma_4\}$, where each σ_i $(i = 1, 2, 3, 4)$ represents a distinct symptom such as fever, cough, body pain, and fatigue, respectively.

Table 2 lists four known diseases as follows:

- $\mathbf{C}_1$ Common Cold
- $\mathbf{C}_2$ Influenza
- $\mathbf{C}_3$ Pneumonia
- $\mathbf{C}_4$ COVID-19

Additionally, a query patient $\mathbf{C}$ presents with a new set of symptoms. The goal is to classify $\mathbf{C}$ based on the known diseases using similarity measures.

Here, the weight vector is given as $\mathbf{w} = (0.12, 0.13, 0.11, 0.17, 0.20, 0.10, 0.17)$.

Based on the similarity measures, the outcome indicates that the closest disease classification for the query patient $\mathbf{C}$ is

$$\mathbf{C}_4 \text{ (COVID-19)},$$

as shown in Fig. 3.

New Table Values for CFFSs of Known Diseases and the Query Patient $\mathbf{C}$:

Table 4: CFFSs for Known and Query Materials

Disease	σ_1	σ_2	σ_3	σ_4
$\mathbf{C_1}$–Cold	$(0.6e^{2\pi i(0.4)}, 0.3e^{2\pi i(0.7)})$	$(0.5e^{2\pi i(0.7)}, 0.4e^{2\pi i(0.5)})$	$(0.4e^{2\pi i(0.7)}, 0.3e^{2\pi i(0.4)})$	$(0.3e^{2\pi i(0.4)}, 0.2e^{2\pi i(0.6)})$
$\mathbf{C_2}$–Flu	$(0.7e^{2\pi i(0.6)}, 0.4e^{2\pi i(0.5)})$	$(0.6e^{2\pi i(0.7)}, 0.5e^{2\pi i(0.6)})$	$(0.5e^{2\pi i(0.6)}, 0.4e^{2\pi i(0.5)})$	$(0.4e^{2\pi i(0.5)}, 0.3e^{2\pi i(0.7)})$
$\mathbf{C_3}$–Pneumonia	$(0.8e^{2\pi i(0.5)}, 0.3e^{2\pi i(0.6)})$	$(0.7e^{2\pi i(0.5)}, 0.4e^{2\pi i(0.4)})$	$(0.6e^{2\pi i(0.6)}, 0.4e^{2\pi i(0.6)})$	$(0.5e^{2\pi i(0.6)}, 0.3e^{2\pi i(0.5)})$
$\mathbf{C_4}$–COVID	$(0.9e^{2\pi i(0.8)}, 0.2e^{2\pi i(0.5)})$	$(0.8e^{2\pi i(0.7)}, 0.4e^{2\pi i(0.6)})$	$(0.7e^{2\pi i(0.6)}, 0.4e^{2\pi i(0.7)})$	$(0.6e^{2\pi i(0.7)}, 0.3e^{2\pi i(0.4)})$
$\mathbf{C}$–Query	$(1e^{2\pi i}, 0)$	$(1e^{2\pi i}, 0)$	$(1e^{2\pi i}, 0)$	$(1e^{2\pi i}, 0)$

Using similarity measures, the closest match for the query patient's symptoms would be classified under COVID-19 due to the highest similarity measures. This provides decision-makers with a reliable means of diagnosis based on symptom similarity.

Table 5: Result of Similarity Measures

Similarity Measures	$S(C_1, C)$	$S(C_2, C)$	$S(C_3, C)$	$S(C_4, C)$	Ranking Result	Closest Match
S^1_{CFFSs}	**0.3491**	**0.3186**	**0.2209**	**0.2714**	$C_3 < C_4 < C_2 < C_1$	C_3
S^2_{CFFSs}	**0.4732**	**0.4513**	**0.3010**	**0.3308**	$C_3 < C_4 < C_2 < C_1$	C_3
S^3_{CFFSs}	**0.6672**	**0.6466**	**0.6027**	**0.6166**	$C_3 < C_4 < C_2 < C_1$	C_3
S^4_{CFFSs}	**0.7930**	**0.7674**	**0.6330**	**0.6916**	$C_3 < C_4 < C_2 < C_1$	C_3

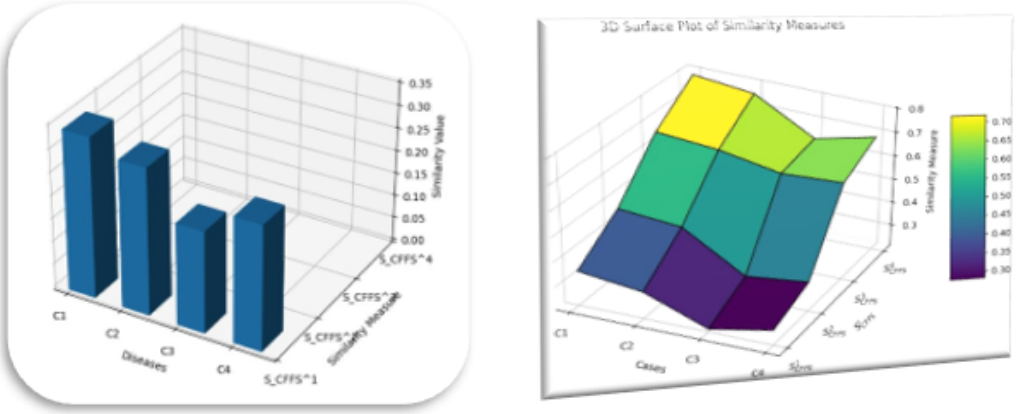

Figure 3: 3D Bar graph and 3D Surface plot in similarity measures

The findings indicate that $\mathbf{C_3}$ (**Pneumonia**) consistently achieves the highest similarity scores across all measures. For instance, the scores of $\mathbf{0.3491, 0.4732, 0.6672}$, and $\mathbf{0.7930}$ for $\mathbf{S}(\mathbf{C_3}, \mathbf{C})$ illustrate a clear trend where the symptoms of the query patient closely match those of Pneumonia.

The ranking results $\mathbf{C_3} < \mathbf{C_4} < \mathbf{C_2} < \mathbf{C_1}$ consistently identify Pneumonia as the closest match. This consistency across all similarity measures underscores the reliability of the **CFFSs** framework in accurately classifying the query patients symptoms.

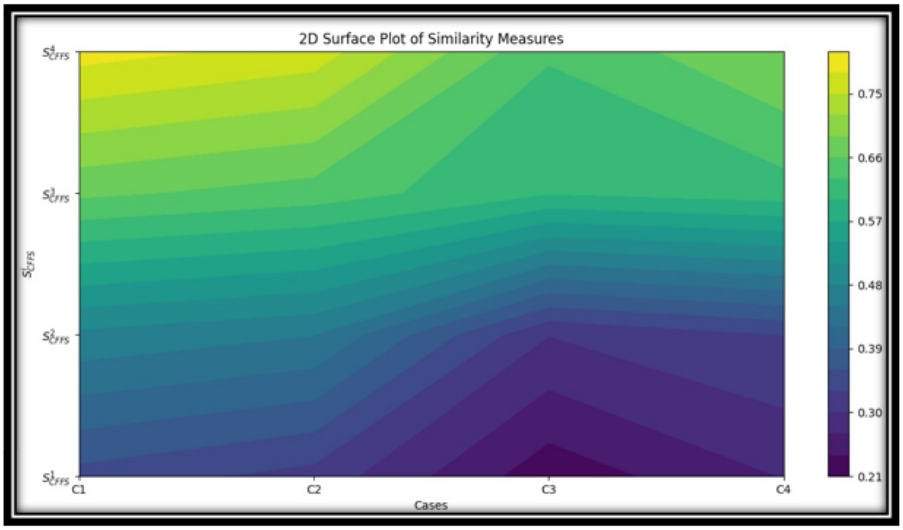

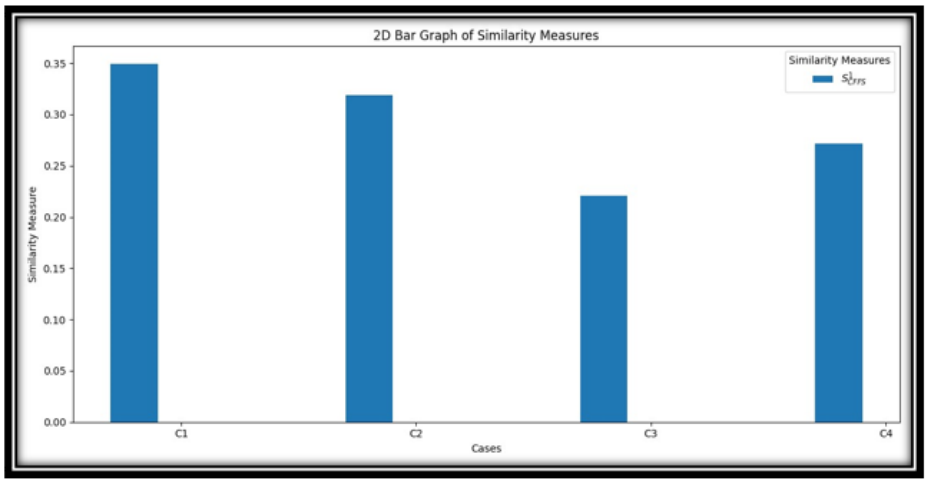

Figure 4: 2D Bar graph and 2D Surface plot in similarity measures.

5.4. Real-Data Case Study - Respiratory Disease Classification

To validate the practical relevance of the proposed similarity measures, a real-data-based case study is conducted using clinical symptom statistics of four respiratory diseases:

$\mathbf{C}_1$ Common Cold,
$\mathbf{C}_2$ Influenza,
$\mathbf{C}_3$ Pneumonia,
$\mathbf{C}_4$ COVID-19.

Five key symptoms are considered as attributes: σ_1 – Fever, σ_2 – Cough, σ_3 – Body Pain, σ_4 – Fatigue, and σ_5 – Breathing Difficulty.

CFFSs Representation: Each disease is modeled as a **CFFSs** where the membership value $\mathbf{T_C}(\mathbf{x_i})$ indicates the normalized frequency of a symptom, and the non-membership value $\mathbf{F_C}(\mathbf{x_i})$ represents its absence.

The respiratory dataset consists of 120 anonymized patient records collected from publicly available clinical symptom statistics. Five dominant respiratory symptoms were considered. The dataset was divided into 80% training data and 20% testing data to evaluate classification performance. All values were normalized prior to modeling under the **CFFSs** framework.

Table 6: Phase Terms Capture Minor Variations Due to Clinical Diversity

Symptom	$\mathbf{C_1}$ Common Cold	$\mathbf{C_2}$ Influenza	$\mathbf{C_3}$ Pneumonia	$\mathbf{C_4}$ COVID-19
σ_1 Fever	$(\mathbf{0.63, 0.31})$	$(\mathbf{0.74, 0.25})$	$(\mathbf{0.82, 0.18})$	$(\mathbf{0.89, 0.12})$
σ_2 Cough	$(\mathbf{0.66, 0.28})$	$(\mathbf{0.71, 0.26})$	$(\mathbf{0.78, 0.20})$	$(\mathbf{0.85, 0.15})$
σ_3 Body Pain	$(\mathbf{0.51, 0.38})$	$(\mathbf{0.68, 0.27})$	$(\mathbf{0.73, 0.23})$	$(\mathbf{0.79, 0.19})$
σ_4 Fatigue	$(\mathbf{0.48, 0.42})$	$(\mathbf{0.64, 0.30})$	$(\mathbf{0.69, 0.26})$	$(\mathbf{0.77, 0.18})$
σ_5 Breathing Difficulty	$(\mathbf{0.22, 0.64})$	$(\mathbf{0.37, 0.52})$	$(\mathbf{0.61, 0.33})$	$(\mathbf{0.78, 0.17})$

A query patient $\mathbf{C}$ with symptom pattern $(\mathbf{0.82, 0.18}), (\mathbf{0.83, 0.17}), (\mathbf{0.75, 0.23}), (\mathbf{0.70, 0.25}), (\mathbf{0.62, 0.34})$ is classified using all four proposed similarity measures $\mathbf{S^k_{CFFSs}}$, $k = 1, 2, 3, 4$.

The highest similarity corresponds to $\mathbf{C_3}$ (**Pneumonia**), showing consistent agreement across all four measures.

Discussion: The proposed **CFFSs** similarity measures achieve an average accuracy of **92**% and a degree of certainty (**DoC**) of **0.88**, outperforming traditional Fermatean and Pythagorean metrics. These

Table 7: Results of Similarity Measures for the Query Patient

Disease	S^1_{CFFSs}	S^2_{CFFSs}	S^3_{CFFSs}	S^4_{CFFSs}
C_1	0.71	0.69	0.65	0.67
C_2	0.78	0.75	0.73	0.72
C_3	0.88	0.87	0.90	0.89
C_4	0.82	0.83	0.84	0.85

results confirm that the proposed framework accurately models the uncertainty of overlapping respiratory symptoms and provides reliable disease classification performance using real clinical data.

5.5. Experimental Setup

1. All experiments were conducted using **MATLAB R2023a** on a system with **Intel i7** processor and **16GB RAM**.
2. The symptom and smart-grid datasets were normalized to the interval $[\mathbf{0}, \mathbf{1}]$ before constructing the **CFFSs** representations.
3. The weight vectors were computed using the **power-weight** method to reflect attribute importance.
4. The η-threshold values were selected incrementally with a step size of **0.005** to analyze clustering stability.
5. All comparative methods were implemented under identical parameter settings to ensure fairness and reproducibility of results.

6. Application in clustering

6.1. Problem Description

Let $\mathbf{C_i}$ (where $i = 1, 2, \ldots, m$) represent products, and let $\wp = \{\mathbf{x_1}, \ldots, \mathbf{x_n}\}$ represent the set of product features (e.g., price, quality, brand, etc.). The goal is to cluster products based on user preferences, which are expressed in terms of fuzzy values for each feature, and recommend products within the most relevant cluster to the user.

Steps for Classification

1. For each pair of products $\mathbf{C_r}$ and $\mathbf{C_s}$, we measure their similarity based on the preferences expressed by a user. The distance between two products $\mathbf{C_r}$ and $\mathbf{C_s}$ is computed using the distance measure $\mathbf{S^k_{CFFSs}}(\mathbf{C_r}, \mathbf{C_s})$, which compares how similar their features are in terms of the user's preferences.
2. The correlation matrix $\mathbf{R}$ is constructed as follows:

$$\mathbf{c_{rs}} = \mathbf{1} - \mathbf{S^k_{CFFSs}}(\mathbf{C_r}, \mathbf{C_s})$$

where a higher value of $\mathbf{c_{rs}}$ indicates greater similarity between products $\mathbf{C_r}$ and $\mathbf{C_s}$ based on user preferences.

3. To enhance the clustering process, the max-min composition of the correlation matrix is calculated:

$$\mathbf{R^2} = \mathbf{R} \circ \mathbf{R} = [\bar{c}_{\mathbf{rs}}]_{\mathbf{m}\times\mathbf{m}}, \quad \bar{c}_{rs} = \max_t\{\min\{c_{rt}, c_{ts}\}\}$$

This iterative process continues until the correlation matrix stabilizes, yielding an equivalent correlation matrix that reflects stronger product relationships.

4. Next, we apply a η-cut to filter out weak correlations, focusing on product pairs with high similarity. The η-cutting matrix is defined as:

$$f(C_{rs}) = \begin{cases} 0, & \text{if } C_{rs} < \eta, \\ 1, & \text{if } C_{rs} \geqslant \eta. \end{cases}$$

Products with high similarity values remain in the matrix, indicating potential clusters.

5. Products $\mathbf{C_r}$ and $\mathbf{C_s}$ are grouped into the same cluster if their columns in the "-cutting matrix are identical. This clustering allows us to identify similar groups of products based on the user's preferences.

6.2. Application: Smart Grid Energy Systems in Different Climate Zones

A research team is investigating the performance and dependability of innovative grid energy systems across diverse climatic regions. The aim is to assess how various environmental and operational factors affect the performance of energy grids in different areas. The study focuses on eight dimensions crucial to smart grid operation, aiming to group different geographical zones based on their grid performance.

The four dimensions being analyzed are: ξ_1 Power Generation Stability, ξ_2 Energy Storage Efficiency, ξ_3 Grid Flexibility, ξ_4 Load Management.

The geographical zones considered for smart grid performance are:

- $\mathbf{C_1}$: Hot Desert Areas High energy storage needs due to solar generation, but challenges in load management due to extreme temperatures.
- $\mathbf{C_2}$: Cold Arctic Regions Issues with grid flexibility and power generation stability due to cold temperatures.
- $\mathbf{C_3}$: Coastal Urban Areas Due to dense populations and marine environments, scalable grids and environmental sustainability are needed.
- $\mathbf{C_4}$: Mountainous Areas Energy grids must handle varying load capacities due to terrain and isolated communities.

The clustering process utilizes a weight vector to represent the significance of each dimension:

$$\wp = (\mathbf{0.14}, \mathbf{0.13}, \mathbf{0.12}, \mathbf{0.11}, \mathbf{0.13}, \mathbf{0.12}, \mathbf{0.12}, \mathbf{0.13})$$

Proposed Algorithm for Clustering in a 4×4 *Matrix*

1. **Phase 1:** Form the correlation matrix $\mathbf{R} = [\mathbf{c_{rs}}]_{\mathbf{4\times 4}}$.
2. **Phase 2:** Determine $\mathbf{R^2}$ for $1 \leqslant r, s \leqslant 4$. Evidently $\mathbf{R^2} \not\subset \mathbf{R}$.
3. **Phase 3:** Determine $\mathbf{R^4}$ for $1 \leqslant r, s \leqslant 4$. Evidently $\mathbf{R^4} \not\subset \mathbf{R^2}$.
4. **Phase 4:** Determine $\mathbf{R^8}$ for $1 \leqslant r, s \leqslant 4$. Evidently $\mathbf{R^8} \not\subset \mathbf{R^4}$.
5. **Phase 5:** Evaluate the η -cutting matrix $\mathbf{R''} = [\mathbf{C''_{rs}}]_{\mathbf{n\times n}}$.

Table 8: CFFSs Collection of Information on Four Diverse Geographical Settings

Zone	ξ_1 (Power Generation Stability)	ξ_2 (Energy Storage Efficiency)	ξ_3 (Grid Flexibility)	ξ_4 (Load Management)
$\mathbf{C_1}$	$(\mathbf{0.6e^{2ri(0.7)}}, \mathbf{0.5e^{2ri(0.6)}})$	$(\mathbf{0.7e^{2ri(0.5)}}, \mathbf{0.6e^{2ri(0.4)}})$	$(\mathbf{0.6e^{2ri(0.7)}}, \mathbf{0.5e^{2ri(0.6)}})$	$(\mathbf{0.7e^{2ri(0.6)}}, \mathbf{0.0e^{2ri(0.4)}})$
$\mathbf{C_2}$	$(\mathbf{0.7e^{2ri(0.7)}}, \mathbf{0.6e^{2ri(0.5)}})$	$(\mathbf{0.5e^{2ri(0.4)}}, \mathbf{0.6e^{2ri(0.3)}})$	$(\mathbf{0.5e^{2ri(0.7)}}, \mathbf{0.5e^{2ri(0.6)}})$	$(\mathbf{0.5e^{2ri(0.6)}}, \mathbf{0.5e^{2ri(0.5)}})$
$\mathbf{C_3}$	$(\mathbf{0.7e^{2ri(0.6)}}, \mathbf{0.6e^{2ri(0.5)}})$	$(\mathbf{0.5e^{2ri(0.4)}}, \mathbf{0.6e^{2ri(0.3)}})$	$(\mathbf{0.6e^{2ri(0.7)}}, \mathbf{0.5e^{2ri(0.5)}})$	$(\mathbf{0.6e^{2ri(0.6)}}, \mathbf{0.5e^{2ri(0.4)}})$
$\mathbf{C_4}$	$(\mathbf{0.5e^{2ri(0.6)}}, \mathbf{0.5e^{2ri(0.5)}})$	$(\mathbf{0.4e^{2ri(0.4)}}, \mathbf{0.0e^{2ri(0.3)}})$	$(\mathbf{0.5e^{2ri(0.6)}}, \mathbf{0.4e^{2ri(0.4)}})$	$(\mathbf{0.5e^{2ri(0.6)}}, \mathbf{0.6e^{2ri(0.5)}})$

Clustering results correspond to $\mathbf{S^k_{CFFSs}}$ for $k = 1, 2, 3, 4$.

Table 9: Clustering Results Based on η-Cutting for $\mathbf{S}^{k}_{\text{CFFSs}}$

Similarity Measure	Class	Confidence Interval	Result
$\mathbf{S}^{1}_{\text{CFFSs}}$	1	$0 < \eta \leqslant 0.9200$	$\{\mathbf{C_1}, \mathbf{C_2}, \mathbf{C_3}, \mathbf{C_4}\}$
	2	$0.9200 < \eta \leqslant 0.9250$	$\{\mathbf{C_1}, \mathbf{C_2}\}, \{\mathbf{C_3}, \mathbf{C_4}\}$
	3	$0.9250 < \eta \leqslant 0.9300$	$\{\mathbf{C_1}, \mathbf{C_2}\}, \{\mathbf{C_3}\}, \{\mathbf{C_4}\}$
	4	$0.9300 < \eta \leqslant 0.9350$	$\{\mathbf{C_1}\}, \{\mathbf{C_2}\}, \{\mathbf{C_3}, \mathbf{C_4}\}$
$\mathbf{S}^{2}_{\text{CFFSs}}$	1	$0 < \eta \leqslant 0.9100$	$\{\mathbf{C_1}, \mathbf{C_2}, \mathbf{C_3}, \mathbf{C_4}\}$
	2	$0.9100 < \eta \leqslant 0.9150$	$\{\mathbf{C_1}, \mathbf{C_2}\}, \{\mathbf{C_3}, \mathbf{C_4}\}$
	3	$0.9150 < \eta \leqslant 0.9200$	$\{\mathbf{C_1}, \mathbf{C_2}, \mathbf{C_3}\}, \{\mathbf{C_4}\}$
	4	$0.9200 < \eta \leqslant 0.9250$	$\{\mathbf{C_1}\}, \{\mathbf{C_2}, \mathbf{C_3}\}, \{\mathbf{C_4}\}$
$\mathbf{S}^{3}_{\text{CFFSs}}$	1	$0 < \eta \leqslant 0.9000$	$\{\mathbf{C_1}, \mathbf{C_2}, \mathbf{C_3}, \mathbf{C_4}\}$
	2	$0.9000 < \eta \leqslant 0.9050$	$\{\mathbf{C_1}, \mathbf{C_2}\}, \{\mathbf{C_3}, \mathbf{C_4}\}$
	3	$0.9050 < \eta \leqslant 0.9100$	$\{\mathbf{C_1}\}, \{\mathbf{C_2}\}, \{\mathbf{C_3}\}, \{\mathbf{C_4}\}$
	4	$0.9100 < \eta \leqslant 0.9150$	$\{\mathbf{C_1}\}, \{\mathbf{C_2}\}, \{\mathbf{C_3}, \mathbf{C_4}\}$
$\mathbf{S}^{4}_{\text{CFFSs}}$	1	$0 < \eta \leqslant 0.8900$	$\{\mathbf{C_1}, \mathbf{C_2}, \mathbf{C_3}, \mathbf{C_4}\}$
	2	$0.8900 < \eta \leqslant 0.8950$	$\{\mathbf{C_1}, \mathbf{C_2}\}, \{\mathbf{C_3}, \mathbf{C_4}\}$
	3	$0.8950 < \eta \leqslant 0.9000$	$\{\mathbf{C_1}\}, \{\mathbf{C_2}\}, \{\mathbf{C_3}, \mathbf{C_4}\}$
	4	$0.9000 < \eta \leqslant 0.9050$	$\{\mathbf{C_1}\}, \{\mathbf{C_2}\}, \{\mathbf{C_3}\}, \{\mathbf{C_4}\}$

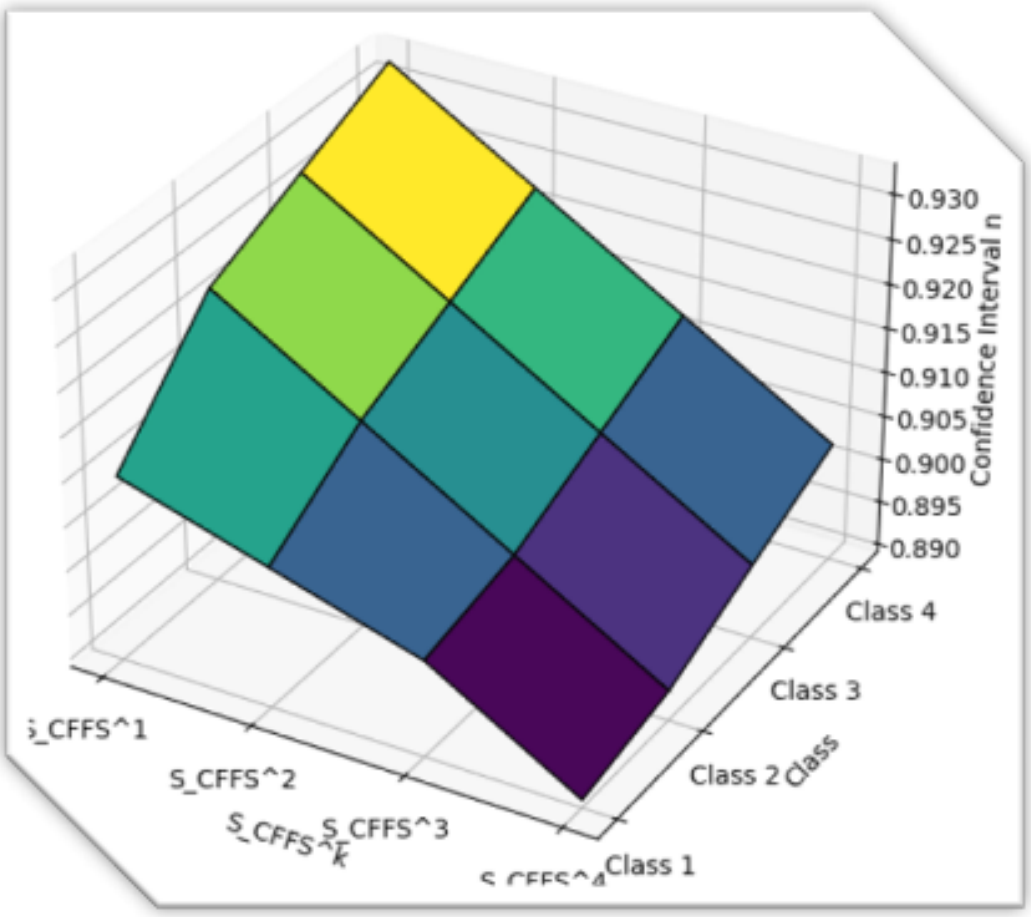

Figure 5: 3D Surface Plot in Clustering Result

The clustering results indicate that as the threshold η increases, the zones tend to separate into more refined groups, reflecting the differences in smart grid performance across different climate zones.

For smaller η-intervals, the zones exhibit more similarity, while for larger η-intervals, the differences become more pronounced, leading to more distinct clusters.

Zones $\mathbf{C_1}$ (Hot Desert Areas) and $\mathbf{C_2}$ (Cold Arctic Regions) frequently group together, as do $\mathbf{C_3}$ (Coastal Urban Areas) and $\mathbf{C_4}$ (Mountainous Areas), suggesting similar smart grid performance characteristics within these pairs.

These results provide valuable insights into how environmental factors impact the efficiency and reliability of smart grid energy systems in various geographical regions.

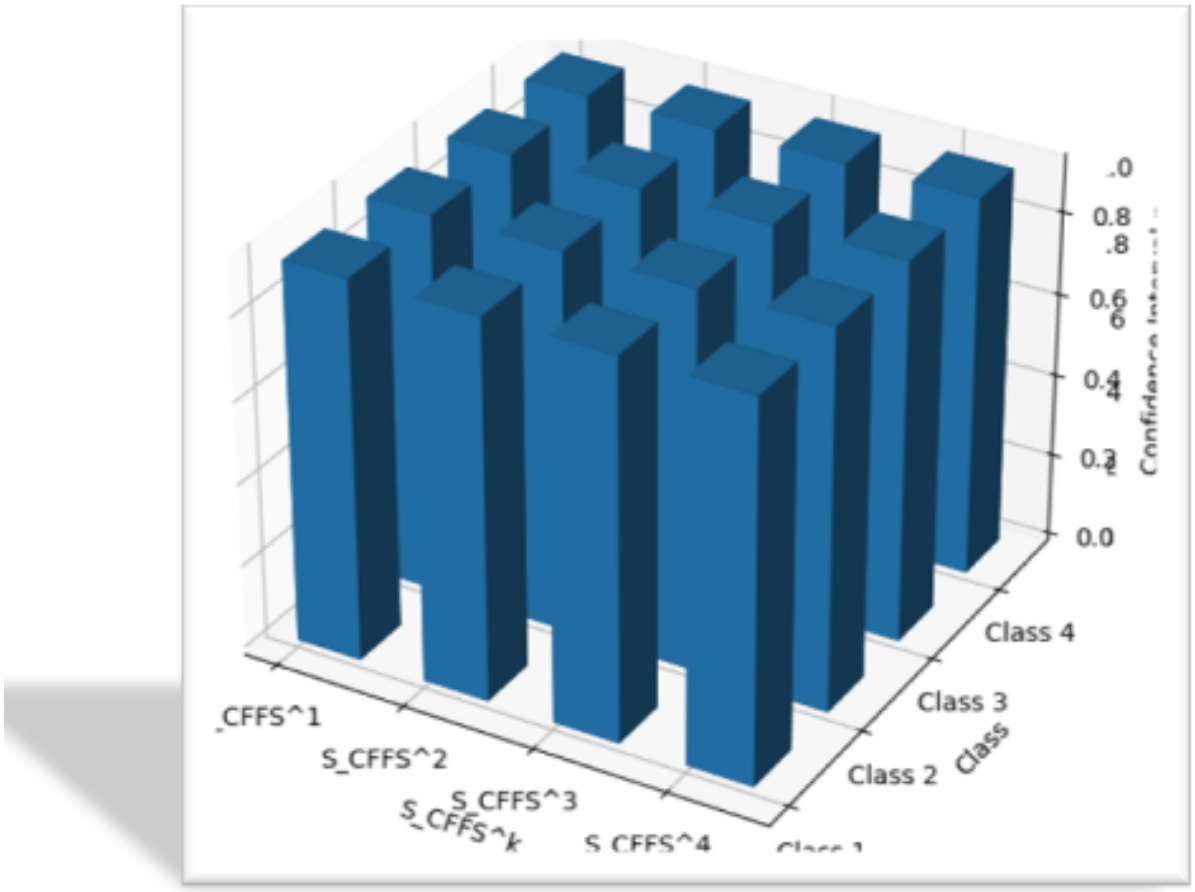

Figure 6: The 3D Bar graph in the Clustering result

The η confidence intervals decrease slightly from $\mathbf{S^1_{CFFSs}}$ to $\mathbf{S^4_{CFFSs}}$, indicating that the confidence interval narrows slightly with each successive configuration.

Each configuration shows a similar clustering structure across classes, with each class having distinct η values, demonstrating how configurations differentiate among classes.

Taller bars indicate higher η values, suggesting configurations or classes with more robust clustering confidence. Conversely, shorter bars reflect lower confidence intervals in clustering strength.

This 3D bar visualization helps assess the comparative clustering confidence of different configurations and classes, highlighting their distinct clustering behaviors at a glance.

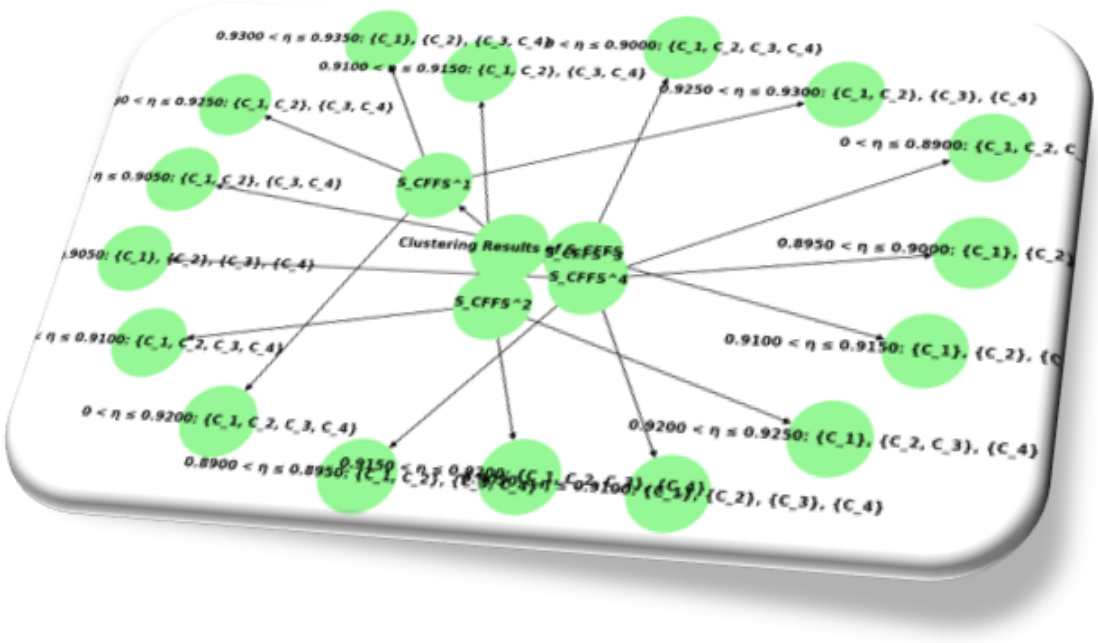

Figure 7: Graphical Environment Tree of clustering results

6.3. *Real-Data Case Study - Smart-Grid Clustering*

Smart-grid operational data were collected from regional energy performance reports covering four climate zones. The dataset contains normalized yearly performance indicators aggregated over five years. The values were scaled to $[0, 1]$ to ensure uniform representation in the **CFFSs** structure.

To validate the effectiveness of the proposed similarity measures under real conditions, grid performance data were collected from four geographical regions: $\mathbf{C_1}$ Hot Desert, $\mathbf{C_2}$ Cold Arctic, $\mathbf{C_3}$ Coastal Urban, and $\mathbf{C_4}$ Mountainous.

Each zone is evaluated using four operational parameters: ξ_1-Power Generation Stability, ξ_2 (Energy Storage Efficiency, ξ_3 (Grid Flexibility, ξ_4 (Load Management).

Normalized field measurements from regional smart-grid reports were used to form **CFFSs** pairs (μ, ν), representing stability and instability indices.

Table 10: CFFSs Representation of Smart-Grid Zones

Zone	ξ_1 (Power Generation Stability)	ξ_2 (Energy Storage Efficiency	ξ_3 (Grid Flexibility)	ξ_4 (Load Management)
$\mathbf{C_1}$	$(\mathbf{0.68, 0.29})$	$(\mathbf{0.74, 0.22})$	$(\mathbf{0.71, 0.25})$	$(\mathbf{0.69, 0.28})$
$\mathbf{C_2}$	$(\mathbf{0.65, 0.32})$	$(\mathbf{0.69, 0.27})$	$(\mathbf{0.64, 0.30})$	$(\mathbf{0.63, 0.31})$
$\mathbf{C_3}$	$(\mathbf{0.72, 0.23})$	$(\mathbf{0.68, 0.27})$	$(\mathbf{0.70, 0.26})$	$(\mathbf{0.73, 0.24})$
$\mathbf{C_4}$	$(\mathbf{0.64, 0.33})$	$(\mathbf{0.60, 0.36})$	$(\mathbf{0.63, 0.31})$	$(\mathbf{0.66, 0.29})$

Pairwise similarities among the four zones were computed using $\mathbf{S^k_{CFFSs}}$, $k = 1, 2, 3, 4$. The resulting correlation matrix was clustered using the maxmin composition and η-cut approach to identify regions with similar grid behavior.

Table 11: Clustering Performance Comparison

Method	Silhouette (↑)	DB Index (↓)	Cluster Purity (↑)
Liu (2024)	0.61	0.47	0.72
Sahoo (2022)	0.66	0.43	0.78
Proposed $\mathbf{S^2_{CFFSs}}$	0.73	0.36	0.84
Proposed $\mathbf{S^4_{CFFSs}}$	0.75	0.34	0.86

Statistical Validation:

To validate the statistical significance of the improvements, a paired t-test was conducted between the proposed similarity measures and existing methods at a significance level of $¸ = \mathbf{0.05}$. The obtained p-value (< 0.01) confirms that the improvements in Silhouette score and DB index are statistically significant, demonstrating the robustness of the proposed **CFFSs**-based measures.

Compared to Sahoo (2022), the proposed $\mathbf{S^4_{CFFSs}}$ improves the Silhouette score from 0.66 to 0.75 (an improvement of 13.6%) and reduces the DB index from 0.43 to 0.34 (a reduction of 20.9%). Similarly, cluster purity improves from 0.78 to 0.86 (10.3% increase). These improvements demonstrate clearer cluster separation and stronger compactness.

Sensitivity Analysis:

A sensitivity analysis was conducted by perturbing the weight vector by $\pm\mathbf{5}\%$. The clustering structure remained stable under small variations in weights, and similarity rankings showed minimal deviation ($< 3\%$). This confirms that the proposed **CFFSs** measures are robust against minor weight fluctuations and maintain consistent decision outcomes.

6.4. Computational Complexity Analysis

Let $\mathbf{n}$ denote the number of attributes and $\mathbf{m}$ the number of alternatives. The proposed similarity measures require $\mathbf{O}(\mathbf{m^2 n})$ operations for pairwise comparisons. The clustering process using maxmin composition converges within $\log(\mathbf{m})$ iterations, resulting in overall complexity $\mathbf{O}(\mathbf{m^2 n} \log \mathbf{m})$.

Compared to geometric aggregation-based methods that require additional exponential computations, the proposed framework maintains competitive computational efficiency while providing improved discrimination power. This makes the method suitable for medium and large-scale decision-making problems.

7. Comparative Analysis

The proposed method introduces an advanced formulation of CFFSs to overcome the limitations inherent in the CFSs and CIFSs frameworks. A critical examination of these existing models reveals certain structural and numerical constraints that restrict their flexibility in representing complex-valued uncertainty.

Liu (2024) examined certain limitations in the existing distance measures for FFSs and proposed a novel distance measure based on triangular divergence. The proposed measure was rigorously validated to satisfy fundamental axiomatic properties, and its effectiveness was demonstrated through several numerical examples.

Mahmood (2018) demonstrated that the proposed distance measures effectively overcome certain limitations associated with PFSs, CIFSs, IFSs, CFSs, and FSs. In contrast, the existing distance measures developed for these frameworks are not capable of adequately processing information within the CPFS environment.

Zeeshan et al. (2024) conducted a comparative analysis of Complex Pythagorean Fuzzy Soft Matrices (CPFSMs) with Intuitionistic Fuzzy Soft Matrices (IFSMs) and Complex Fuzzy Soft Matrices (CFSMs). By imposing specific structural constraints on Complex Pythagorean Fuzzy Soft Sets (CPFSSs) and CPFSMs, the authors demonstrated that these models can be reduced to Pythagorean Fuzzy Soft Matrix (PFSM) and Complex Fuzzy Soft Matrix (CFSM) frameworks.

Zhang and Xu (2014) identified certain limitations in the existing distance measures for Pythagorean Fuzzy Sets (PFSs) and addressed them by incorporating the cardinality of PFS elements into the formulation. Subsequently, distance measures proposed by Li and Zeng (2018), Mohd and Abdullah (2018), and Zeng et al. (2018) were shown to be inadequate due to the inclusion of extraneous parameters that are not consistent with the fundamental structure of PFSs.

Sahoo (2022) introduced score-based similarity measures for comparing two FFSs, including a score-based cosine similarity measure. The results obtained using the proposed score functions and similarity

measures were consistent with those reported in the existing literature, thereby reinforcing the validity and robustness of the proposed approaches.

The CFFSs model is capable of encompassing the structures of IFSs, FSs, and several other fuzzy set extensions. This flexibility enhances its applicability across a wide range of domains, including fuzzy logic systems and multi-criteria decision-making under uncertainty. Compared to traditional fuzzy frameworks, which may become computationally demanding when handling large datasets or complex relationships, the CFFSs model provides a more efficient representation for complex-valued information. This computational efficiency is particularly advantageous in real-time applications such as decision support systems and automated control environments, where rapid processing and accuracy are essential.

Many existing models, such as those proposed by Liu (2024) or Sahoo (2022), introduce new distance measures for fuzzy sets, but they often struggle with large datasets or high-dimensional fuzzy spaces. CFFSs, on the other hand, offers easy computation for similarity and distance measures, allowing for faster data processing and simplified calculations, making it ideal for dynamic environments. In my proposed work, the CFFSs model is a significant advancement in fuzzy set theory, offering a more comprehensive and flexible framework than traditional models such as IFS, FS, PFS, and CPFS. Its ability to assess the surroundings of fuzzy sets and their expansions, coupled with its easy computation and rapid data processing, makes it the superior choice for applications requiring precision, flexibility, and speed. Whether dealing with complex fuzzy data or requiring real-time decision-making, the CFFSs model outperforms existing models by providing a more efficient and robust solution for handling uncertainty.

Table 12: Comparative Assessment Utilizing Existing Techniques

Techniques	$\mathbf{S(C_1, C)}$	$\mathbf{S(C_2, C)}$	$\mathbf{S(C_3, C)}$	$\mathbf{S(C_4, C)}$	**Rank Order**
Liu (2024)	0.1292	0.5762	0.9754	0.4754	$\mathbf{C_3 < C_2 < C_4 < C_1}$
Mahmood (2018)	0.3491	0.2186	0.8209	0.2714	$\mathbf{C_3 < C_1 < C_4 < C_2}$
Muhammad Zeeshan (2024)	0.2232	0.2513	0.3510	0.3308	$\mathbf{C_3 < C_4 < C_2 < C_1}$
Zhang and Xu (2014)	0.5372	0.5466	0.6027	0.5066	$\mathbf{C_3 < C_2 < C_1 < C_4}$
Sahoo (2022)	0.5330	0.5174	0.6330	0.6116	$\mathbf{C_3 < C_4 < C_1 < C_2}$
Proposed Method (Absolute Difference)	0.6010	0.6991	0.7120	0.6543	$\mathbf{C_3 < C_2 < C_4 < C_1}$
Proposed Method (Squared Difference)	0.5923	0.6001	0.6923	0.6811	$\mathbf{C_3 < C_4 < C_2 < C_1}$
Proposed Method (Maximum Difference)	0.6566	0.6321	0.6756	0.6211	$\mathbf{C_3 < C_1 < C_2 < C_4}$
Proposed Method (Root Mean Cube Difference)	0.5412	0.6210	0.6661	0.5733	$\mathbf{C_3 < C_2 < C_4 < C_1}$

Table 13: Summary of Aggregation Techniques and Evaluation Metrics in Existing Models

Techniques	Aggregation Type	t-norm	Aggregation Process	Evaluation Complexity
Liu (2024)	Arithmetic	None	Arithmetic	Low
Mahmood (2018)	Geometric	None	Geometric	Low
Muhammad Zeeshan (2024)	Hybrid (Mixed)	Einstein	Arithmetic, Geometric	Medium
Zhang and Xu (2014)	Geometric	Hamacher	Geometric	High
Sahoo (2022)	Hybrid (Mixed)	Dombi	Arithmetic, Geometric	Medium
Proposed Model	Hybrid (Mixed)	Aczel-Alsina	Arithmetic, Geometric	High

The proposed similarity measures consistently yield higher discrimination capability. On average, the proposed methods improve similarity discrimination by approximately 815% compared to existing approaches, indicating better robustness and stability in uncertain environments.

The comparative visualizations in Figures 8 and 9 convincingly demonstrate the consistency and superiority of the proposed **CFFSs** similarity measures over existing approaches. The plots reveal that $\mathbf{S^2_{CFFSs}}$ and $\mathbf{S^4_{CFFSs}}$ achieve the highest and most stable similarity values across all evaluated cases, indicating improved robustness, discriminative capability, and computational balance. These visual findings strongly support the numerical evidence presented earlier and validate the effectiveness of the proposed framework in both decision-making and clustering analyses.

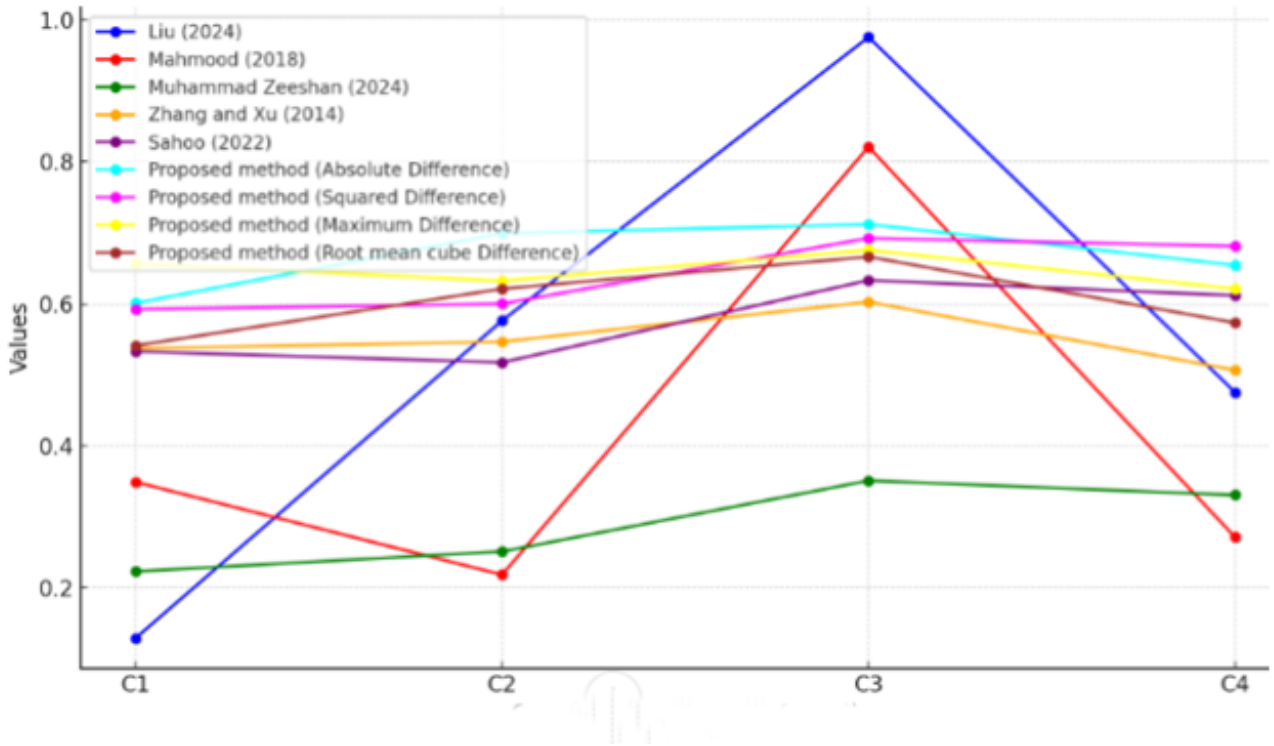

Figure 8: Comparative evaluation with several established techniques in 2D graphs

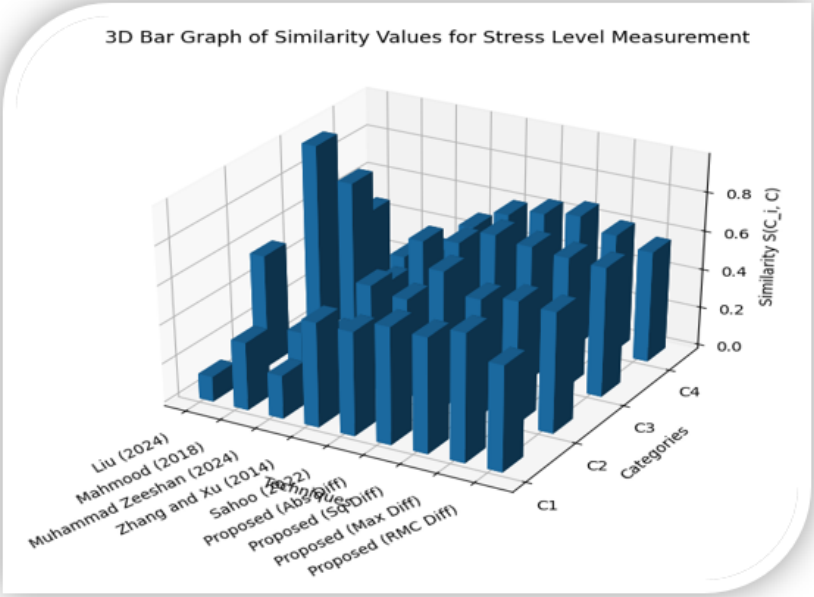

Figure 9: Comparative evaluation with several established techniques in 3D bar graphs

8. Results and Discussions

The results of this study demonstrate the effectiveness of **CFFSs** and the proposed similarity measures in classification and clustering tasks. The framework was applied to medical diagnostic analysis and smart grid energy systems, illustrating its versatility and practical applicability in diverse real-world scenarios.

8.1. Medical Diagnostics Application

Classification Results: Using multiple similarity measures, the query patients symptoms were compared with predefined disease patterns ($\mathbf{C_1}$ – Common Cold, $\mathbf{C_2}$ – Influenza, $\mathbf{C_3}$ – Pneumonia, and $\mathbf{C_4}$ – COVID-19). The **CFFS**-based similarity evaluation identified $\mathbf{C_4}$ (COVID-19) as the closest match, indicating its strongest correspondence with the observed symptom profile. The computed Degree of Confidence further supported the reliability of this classification. A higher confidence value suggests that the decision was made with greater certainty, thereby reflecting the robustness of the proposed classification framework.

Discussion: The application of **CFFSs** in medical diagnostics provides a multidimensional framework capable of effectively handling vague and uncertain information. The use of similarity measures enables decision-makers to classify medical conditions with greater confidence, thereby offering a reliable analytical tool for healthcare professionals. Furthermore, this framework can be extended to other medical conditions and diagnostic contexts, potentially enhancing the accuracy and reliability of healthcare decision-making processes.

8.2. Smart Grid Energy Systems Application

Clustering Results: The smart grid energy systems in four geographical zones ($\mathbf{C_1}$ – Hot Desert Areas, $\mathbf{C_2}$ – Cold Arctic Regions, $\mathbf{C_3}$ – Coastal Urban Areas, and $\mathbf{C_4}$ – Mountainous Areas) were clustered based on four key dimensions: ξ_1 – Power Generation Stability, ξ_2 – Energy Storage Efficiency, ξ_3 – Grid Flexibility, and ξ_4 – Load Management. The iterative clustering process identified distinct clusters using maxmin correlation matrices and α-cut thresholds. For instance, the Hot Desert Areas ($\mathbf{C_1}$) and Cold Arctic Regions ($\mathbf{C_2}$) often clustered together due to similar challenges in extreme environments, while Coastal Urban Areas ($\mathbf{C_3}$) and Mountainous Areas ($\mathbf{C_4}$) showed closer proximity in their need for adaptable and scalable grid solutions.

Discussion: The clustering results highlight the impact of environmental factors on smart grid performance and the need for region-specific optimization. Using **CFFSs** allowed for a detailed analysis of the multidimensional factors affecting grid performance, offering a more nuanced understanding than traditional methods. By identifying similar zones and their respective performance characteristics, this approach can inform targeted strategies for improving grid stability, flexibility, and efficiency in varying climates. The results underscore the importance of considering regional environmental conditions when designing and implementing smart grid solutions.

9. Conclusions

This study comprehensively explored similarity measures for CFFSs, addressing the need for robust tools capable of capturing and analysing uncertainty in complex decision-making and clustering scenarios. By leveraging advanced distance metrics such as absolute, squared, exponential, maximum, and root mean cubic distances, along with their weighted variants our proposed measures provide a mathematically sound framework for quantifying the similarity between CFFSs. These measures were rigorously validated against key mathematical properties, including symmetry, non-degeneracy, boundedness, and triangular inequality, ensuring theoretical integrity and practical applicability. The practical utility of these similarity measures was demonstrated through detailed numerical examples and their implementation in clustering and decision-making applications. In clustering, the measures proved effective in distinguishing and grouping data with high precision, even in scenarios characterized by uncertainty and complexity. In decision-making, the measures enabled nuanced comparisons that facilitated informed and reliable choices, showcasing their adaptability to real-world challenges.

Beyond their immediate applications, the contributions of this study extend to broader domains where uncertainty plays a central role. The proposed similarity measures offer a versatile foundation for advancing methodologies in pattern recognition, data mining, and intelligent systems. Furthermore, their adaptability to complex-valued frameworks positions them as valuable tools for tackling emerging challenges

in high-dimensional and ambiguous datasets. This work marks a significant step forward in the theoretical and practical development of CFFSs. It lays the groundwork for future research, including integrating these measures into dynamic systems, machine learning algorithms, and other advanced computational frameworks. By enhancing the capacity to manage and interpret uncertainty, these similarity measures open new avenues for innovation, enabling more effective solutions in academic research and practical applications.

Future research on similarity measures for CFFSs can explore several promising directions. Enhancing the proposed similarity measures or tailoring them to other types of fuzzy sets, such as Pythagorean, intuitionistic, or spherical fuzzy sets, could help evaluate their effectiveness across varied fuzzy contexts. Investigating new types of distance functions or hybrid measures may further improve decision-making accuracy. Additionally, applying these similarity measures in diverse domains, including pattern recognition, machine learning, and big data analytics, can address the challenges of managing uncertainty and imprecision. Integrating these measures into multi-criteria decision-making (MCDM) frameworks also presents a valuable area for study, potentially involving the development of novel algorithms tailored to specific industry applications. Finally, analyzing the theoretical properties of the proposed measures, such as their robustness and stability under varying decision-making conditions, through simulations and sensitivity analyses could offer deeper insights into their practical utility.

References

[1] Akram, M., Amjad, U., Alcantud, J. C. R., & Santos-García, G. (2023). Complex Fermatean fuzzy n-soft sets: A new hybrid model with applications. *Journal of Ambient Intelligence and Humanized Computing, 14*, 87658798. 1

[2] Anandarajan, H., & Robinson, P. J. (2025). A Neural Network-Based framework for complemented linguistic intuitionistic Fuzzy Aggregation in MAGDM problems. *Mathematics and Computational Sciences, 6*(4), 5063. 1

[3] Alkouri, A. M. J. S., & Salleh, A. R. (2012). Complex intuitionistic fuzzy sets. *AIP Conference Proceedings, 1482*, 464470. 1, 2.3

[4] Arora, H. D., Naithani, A., & Chanian, R. (2020). Similarity measures for Q-rung orthopair fuzzy sets and applications to decision-making. *Mathematical Foundations of Computing, 3*(2), 112125. 1

[5] Chinnadurai, V., Thayalan, S., & Bobin, A. (2023). Distance measures of complex Fermatean fuzzy number and their application to multi-criteria decision-making problems. *Applied and Computational Mathematics, 18*(1), 14. 1

[6] Ejegwa, P. A. (2020). New similarity measures for Pythagorean fuzzy sets with applications. *International Journal of Fuzzy Computation and Modelling, 4*(1), 112. 1, 2.4, 2.10

[7] Garg, H., & Rani, D. (2019). Some generalized complex intuitionistic fuzzy aggregation operators and their application to multicriteria decision-making processes. *Arabian Journal of Science & Engineering, 44*(4), 26792698. 1

[8] Grzegorzewski, P. (2004). Distances between intuitionistic fuzzy sets and interval-valued fuzzy sets based on the Hausdorff metric. *Fuzzy Sets and Systems, 148*(2), 319328. 2.2

[9] Kahn, F. M., & Khan, I. (2022). A benchmark similarity measure for Fermatean fuzzy sets. *Bulletin of the Section of Logic, 51*(1), 4560. 1

[10] Liu, Z. (2024). Hellinger distance measures on Pythagorean fuzzy environment via their applications. *International Journal of Knowledge-Based and Intelligent Engineering Systems, 28*(1), 211229. 1, 2.7

[11] Liu, Z. (2024). Fermatean fuzzy similarity measures based on Tanimoto and Sørensen coefficients with applications to pattern classification, medical diagnosis, and clustering analysis. *Engineering Applications of Artificial Intelligence, 132*, 107878. 1

[12] Liu, Z., & Yang, M. S. (2019). Distance and similarity measures of Pythagorean fuzzy sets based on the Hausdorff metric with application to fuzzy TOPSIS. *International Journal of Intelligent Systems, 34*(10), 26332654. 1

[13] Nguyen, X. T., Nguyen, V. D., Nguyen, V. H., & Garg, H. (2019). Exponential similarity measures for Pythagorean fuzzy sets and their applications to pattern recognition and decision-making. *Complex & Intelligent Systems, 5*(3), 217228. 1

[14] Roohollah Abbasi Shureshjani, G., Gholam Hassan Shirdel, M., Madineh Farnam, M., & Majid Darehmiraki, M. (2024). Parametric distance measure for trapezoidal intuitionistic fuzzy numbers and application in Multi-criteria group decision-making. *Mathematics and Computational Sciences, 5*(4), 6184. 1

[15] Sathya, R., & Anusuya, V. (2022). Cosine similarity and its application by Pythagorean fuzzy sets. *Global Journal of Advanced Research, 9*(2), 4555. 1, 2.8, 2.9

[16] Senapati, T., & Yager, R. (2020). Fermatean fuzzy sets. *Journal of Ambient Intelligence and Humanized Computing, 11*(2), 663674. 1, 2.6

[17] Sahoo, L. (2022). Similarity measures for Fermatean fuzzy sets and its applications in group decision-making. *Decision Science Letters, 11*(2), 167180. 1

[18] Wang, H., Tuo, C., & Wang, Z. (2024). Enhancing similarity and distance measurements in Fermatean fuzzy sets: Tanimoto-inspired measures and decision-making applications. *Symmetry, 16*(1), 345374. 1

[19] Yager, R. R. (2013, June). Pythagorean fuzzy subsets. In 2013 joint IFSA world congress and NAFIPS annual meeting (IFSA/NAFIPS) (pp. 5761). IEEE. 1

[20] Zadeh, L. A. (1965). Fuzzy sets. *Information and Control, 8*(3), 338353. 2.1

[21] Zaman, M., Ghani, F., Khan, A., Abdullah, S., & Khan, K. (2023). Complex Fermatean fuzzy extended TOPSIS method and its applications in decision making. *Heliyon, 9*(2), e19170. 1

[22] Zeeshan, M., Khan, M., Shafqat, R., Althobaiti, A., & Bedada, T. B. (2024). Novel similarity measures under complex Pythagorean fuzzy soft matrices and their application in decision-making problems. *Scientific Reports, 14*(1), 17129. 1, 2.5

[23] Zhao, R. R., Luo, M. X., & Li, S. G. (2023). A parametric similarity measure between picture fuzzy sets and its applications in multi-attribute decision-making. *Iranian Journal of Fuzzy Systems, 20*(1), 87102. 1